

Faculteit Industriële
Ingenieurswetenschappen

master in de industriële wetenschappen: chemie

Masterthesis

Textile Transformations: Upcycling Waste rPET-Textiles with Elongated, Bio-based Soft Blocks into High-Value TPC Materials

Nina Van Gelder

Scriptie ingediend tot het behalen van de graad van master in de industriële wetenschappen: chemie

PROMOTOR :

Prof. dr. Anton GINZBURG

PROMOTOR :

Prof. dr. Louis PITET

COPROMOTOR :

Ms. Victoria SAFIN TIMUROVA

Gezamenlijke opleiding UHasselt en KU Leuven



Universiteit Hasselt | Campus Diepenbeek | Faculteit Industriële Ingenieurswetenschappen | Agoralaan Gebouw H - Gebouw B | BE 3590 Diepenbeek

Universiteit Hasselt | Campus Diepenbeek | Agoralaan Gebouw D | BE 3590 Diepenbeek
Universiteit Hasselt | Campus Hasselt | Martelarenlaan 42 | BE 3500 Hasselt



2023
2024

Faculteit Industriële Ingenieurswetenschappen

master in de industriële wetenschappen: chemie

Masterthesis

Textile Transformations: Upcycling Waste rPET-Textiles with Elongated, Bio-based Soft Blocks into High-Value TPC Materials

Nina Van Gelder

Scriptie ingediend tot het behalen van de graad van master in de industriële wetenschappen: chemie

PROMOTOR :

Prof. dr. Anton GINZBURG

PROMOTOR :

Prof. dr. Louis PITET

COPROMOTOR :

Ms. Victoria SAFIN TIMUROVA



KU LEUVEN

Preface

It is with great pleasure that I present my master's thesis, titled "Textile Transformations: Upcycling Waste rPET-Textiles with Elongated, Bio-based Soft Blocks into High-Value TPC Materials". This thesis has been written over the course of six months to fulfill the requirements for the degree of Master of Chemical Engineering Technology. Throughout my academic career, I have developed an interest in polymer sciences, packaging materials, and sustainability in the industry. An internship at UHasselt AFP Group was a natural choice as it seamlessly combines these interests.

During this period, I have gained not only technical skills but also learned the value of patience and the importance of trusting the process. I would first like to extend my deepest gratitude to Prof. Dr. Pitet, L. M., and Prof. Dr. Ginzburg, A. for giving me this opportunity, taking the time to guide me through this journey, and sharing their experiences and knowledge with me. Secondly, I would like to thank Victoria Safin for her kindness, patience, and guidance. I am truly honored to have had the opportunity to work alongside you. Lastly, I would like to thank my partner and best friend, Wouter, for his love and unconditional support throughout my academic career.

Table of Contents

| | |
|---|-----------|
| Preface | 1 |
| Table of Contents..... | 3 |
| List of Tables | 5 |
| List of Figures | 7 |
| Abstract..... | 11 |
| Abstract in Dutch..... | 13 |
| 1 Introduction | 15 |
| 1.1 General introduction..... | 15 |
| 1.2 Problem statement..... | 15 |
| 1.3 Research goals..... | 17 |
| 1.4 Master's thesis content..... | 18 |
| 2 Literature study | 19 |
| 2.1 Recycling of polyethylene terephthalate | 19 |
| 2.1.1 Polyethylene terephthalate (PET)..... | 19 |
| 2.1.2 Recycling and waste management..... | 21 |
| 2.1.3 Depolymerization of PET | 23 |
| 2.1.4 Upcycling..... | 25 |
| 2.2 Thermoplastic elastomers..... | 26 |
| 2.2.1 Sustainable hard segment..... | 27 |
| 2.2.2 Sustainable soft segment..... | 28 |
| 2.2.3 Elongated soft segment..... | 30 |
| 3 Materials and methods..... | 37 |
| 3.1 Materials..... | 37 |
| 3.1.1 Reagents and chemicals..... | 37 |
| 3.1.2 Equipment..... | 38 |
| 3.2 Methods | 38 |
| 3.2.1 Oligomer synthesis..... | 38 |
| 3.2.2 Polymer synthesis..... | 40 |
| 3.2.3 Characterization of the polymers..... | 42 |
| 4 Results and discussion | 45 |
| 4.1 Oligomer synthesis..... | 45 |
| 4.1.1 ¹ H-NMR..... | 46 |
| 4.1.2 GPC..... | 50 |
| 4.1.3 MALDI-TOF..... | 52 |

| | | |
|--------|--|-----------|
| 4.2 | Polymer synthesis..... | 53 |
| 4.2.1 | ¹ H-NMR..... | 54 |
| 4.2.2. | ¹³ C-NMR..... | 58 |
| 4.2.3 | GPC..... | 60 |
| 4.3 | Mechanical testing..... | 62 |
| 4.3.1 | DSC..... | 62 |
| 4.3.2 | Tensile testing..... | 64 |
| 4.3.3 | Adhesion tests..... | 65 |
| 5 | Conclusion..... | 67 |
| | <i>Oligomer synthesis.....</i> | <i>67</i> |
| | <i>Polymer synthesis.....</i> | <i>67</i> |
| | <i>Characterization of Polymers.....</i> | <i>67</i> |
| | References | 69 |
| | Appendix | 75 |
| | Appendix 1 | 75 |
| | Appendix 2 | 75 |
| | Appendix 3 | 76 |
| | Appendix 4 | 77 |
| | Appendix 5 | 77 |

List of Tables

| | |
|---|----|
| Table 1: Parameters for the oligomer synthesis using succinic acid without the addition of a catalyst..... | 39 |
| Table 2: Parameters for the oligomer synthesis using succinic acid with the addition of a catalyst | 39 |
| Table 3: Parameters for the oligomer synthesis using dimethyl succinate | 39 |
| Table 4: Integrals of peaks from ^1H -NMR spectra of oligomers with different temperatures and reaction times | 48 |
| Table 5: Ratio values calculated from ^1H NMR spectra of the oligomers shown in Figure 30. | 49 |
| Table 6: Ratio values calculated from the ^1H -NMR spectra of the oligomers with the addition of a catalyst..... | 49 |
| Table 7: Ratio values calculated from the ^1H -NMR spectra of the oligomers used for polymer synthesis | 50 |
| Table 8: ^1H -NMR integral values of the peaks marked in Figure 34, from polymers with 60wt% of soft block added..... | 56 |
| Table 9: Values for molecular mass from SEC Measurements from light scattering and refractive index detection for polymer samples | 60 |
| Table 10: Summary of thermal characterization of the polymers synthesized | 62 |
| Table 11: Summary of the mechanical properties of the selected polymer samples derived from 2:1 FADD:SA oligomers and 3:2 FADD:SA oligomers | 64 |
| Table 12: Values measured of sample POLY-F2S1k-90wt%, scotch tape and a sticky note during a peel adhesion test | 65 |
| Table 13: Summary of thermomechanical analysis results of TPCs | 67 |
| Table 14: Summary of tensile test results on the TPCs..... | 68 |
| Table 15: Summary of peel adhesion test results | 68 |
| Table 16: Ratio values calculated from ^1H NMR spectra of the oligomers with varying reaction times (1hours-7hours) | 75 |
| Table 17: ^1H -NMR accompanying resulting values of spectra given in Figure 37. | 77 |

List of Figures

| | |
|--|----|
| Figure 1: Share of plastics treated by waste management category, after disposal of recycling residues and collected litter in 2019. Modified from [10]. | 16 |
| Figure 2: World thermoplastic resin capacity in the year 2008 [17]. | 17 |
| Figure 3: Structure of PET repeating unit | 19 |
| Figure 4: Reaction scheme for the synthesis of PET. BHET formed by TPA and EG (a), or DMT and EG (b), and polymerized to PET (c) ([25], [24], p. 66). | 20 |
| Figure 5: Schematic overview of the different recycling pathways and their predominant problems, modified from [40]. | 22 |
| Figure 6: Schematic overview of the plastic post-consumer waste management in 2020 in EU27+3([39], p. 27) | 23 |
| Figure 7: Diverse depolymerization/upcycling strategies for rPET, using (a) hydrolysis, (b) glycolysis, (c) alcoholysis, and (d) aminolysis ([58], p. 1749) | 25 |
| Figure 8: Overview of rPET converted to higher-value FRPs through two different routes ([61], p. 1008). | 26 |
| Figure 9: Categories of polymer materials [68] | 27 |
| Figure 10: Structure of PBT-PTHD copolymer and schematic overview of chain composition of the different samples ([74], p. 3) | 28 |
| Figure 11: (a) Polymerization reaction scheme of Priamine 1075 with Pripol 1009 (b.) Illustration of the supramolecular structure due to the long entangled main chains, multiple dangling chains, abundant van der Waals bonds, and minor hydrogen bonds, attributable to its stretchability and self-healing efficiency. Modified from([66], p. 6721) | 28 |
| Figure 12: The Complementary synthetic pathways to high-performance TPCs by combining rPET with FADD ([4], p. 352) | 29 |
| Figure 13: Flory-Huggins phase diagram for components with equal degrees of polymerization [71]. | 30 |
| Figure 14: Property boundaries set by different soft block (a, b, and c) molar mass, made with biorender.com | 30 |
| Figure 15: Schematic representation of distribution between a fixed wt% soft block and different length of hard block (modified from [84], p. 606) | 31 |
| Figure 16: Reaction mechanism for the synthesis of PBT/PEG block copolymer(modified from: [84], p. 605). | 32 |
| Figure 17: Synthesis of TPC from DMT, 4G, and PTMEG (modified from: [87], p. 729). | 32 |
| Figure 18: Stress-strain curves of TPC as a function of the 4GT content ([87]p. 739) | 33 |
| Figure 19: Synthetic route of PBT-PBBS copolyester([83], p. 2). | 34 |
| Figure 20: Simplified reaction mechanism for oligomer synthesis from fatty acid dimer diol (FADD) and succinic acid (SA), made with Biorender.com | 35 |
| Figure 21: Simplified reaction mechanism for polymer synthesis from the elongated oligomer and waste textile PET (rPET), made with Biorender.com | 35 |
| Figure 22: Structural formula of the main isomer in Pripol 1009-LQ-(GD), made with Chemdraw. | 37 |
| Figure 23: Experimental setup for synthesizing oligomer in a one-pot polycondensation, made with Biorender.com | 39 |
| Figure 24: Experimental setup polymer synthesis made with Biorender.com | 41 |
| Figure 25: Precipitation and drying process of the polymer overview, made with Biorender.com | 41 |
| Figure 26: Dimensions of tensile specimen in mm [modified from [91]] | 42 |
| Figure 27: Peel adhesion test set up with different parts marked (modified from [92]) | 43 |

| | |
|---|----|
| Figure 28: Representation of reaction for the synthesis of the oligomer with FADD and SA, made with Biorender.com..... | 45 |
| Figure 29: ¹ H-NMR spectra of pure SA, pure FADD, and, a 2:1 ratio oligomer with corresponding structures | 46 |
| Figure 30: ¹ H-NMR spectra of oligomers with different temperatures (190 and 220°C) and reaction times (1h and 4h) of the 2:1 FADD:SA ratio, and 3:2 FADD:SA ratio oligomers..... | 47 |
| Figure 31: Schematic representation of the oligomer structure with protons for further calculations marked. | 48 |
| Figure 32: Molecular weight distributions of selected samples from GPC measurements. (upper) 2:1 FADD:SA ratio oligomers (lower) 3:2 FADD:SA ratio oligomers..... | 50 |
| Figure 33: Molecular weight distributions of selected samples from GPC measurements, differing between oligomers synthesized without a catalyst (dotted line), and an equivalent oligomer with the addition of a catalyst (full line) | 51 |
| Figure 34: Molecular weight distributions measured with MALDI-TOF of sample F2S1k-(3+2)h-(190-220) | 52 |
| Figure 35: Synthesis of TPC from FADD:SA-oligomer and Textile rPET, made with Biorender.com | 53 |
| Figure 36: ¹ H-NMR spectra of (top)a formed TPC with corresponding structure and marked peaks, (middle) the used oligomer, and (bottom) the waste textile PET material..... | 54 |
| Figure 37: Representative ¹ H-NMR spectra of polymers synthesized from (top)F2S1 oligomer without catalyst and, (bottom) F2S1 oligomer with addition of catalyst | 55 |
| Figure 38: Representative ¹ H-NMR spectra of polymers synthesized from rPET with 2:1 FADD:SA ratio oligomers..... | 56 |
| Figure 39: Representative ¹ H-NMR spectra of polymers synthesized from rPET with 3:2 FADD:SA ratio oligomers..... | 57 |
| Figure 40: Soft block of the TPC with all possible sequences shown in one figure all together. | 58 |
| Figure 41: Selected ¹³ C-NMR spectra, with the key regions from the different segment distributions marked as shown in accompanying polymer structure, with T= terephthalic acid, E= ethylene glycol, F= fatty acid dimer diol, and S= succinic acid..... | 58 |
| Figure 42: Summary of ¹³ C-NMR spectra of TPCs with magnifications of the key areas for sequence analysis. (left) represents the sequences FTE, FTF, ETE, and ETF, which can be used for hard block length calculations. (right) represents the sequences FSE, FSF, ESE, and ESF, which proves the presence of transesterification. | 59 |
| Figure 43: GPC data for polymers from (left) 2:1 ratio oligomers and (right) 3:2 ratio oligomers as soft blocks in different wt% | 60 |
| Figure 44: Thermograms of the polymers with 2:1 FADD:SA oligomer and 3:2 FADD:SA oligomer as soft blocks, showing (a) the cooling cycle (10°C/min) and (b) the second heating cycle (10°C/min). The graphs have been vertically adjusted for better clarity. Arrows mark the approximate locations of thermal transitions..... | 62 |
| Figure 45: Appearance of synthesized polymers (left) with a 60 wt% of soft block (right) with a 80 wt% of soft block | 63 |
| Figure 46: Summary of the stress-strain curves of the selected polymer samples derived from (left) 2:1 FADD:SA ratio oligomers (right) 3:2 FADD:SA ratio oligomers | 64 |
| Figure 47: Peel adhesion test on POLY-2:1-90wt%, and for reference on scotch tape and a post-it note. | 65 |
| Figure 48: ¹ H-NMR spectra of oligomers with and without addition of the catalyst. From top to bottom: (a) 2:1 FADD:SA ratio oligomer without catalyst (b) 2:1 FADD:SA ratio oligomer with catalyst (c) 3:2 FADD:SA oligomer without catalyst (d) 3:2 FADD:SA oligomer with catalyst..... | 75 |
| Figure 49: ¹ H-NMR spectra of the oligomers used for the polymer synthesis (top) 2:1 FADD:SA ratio oligomer (bottom) 3:2 FADD:SA ratio oligomer | 76 |

| | |
|---|----|
| Figure 50: TPCs synthesized from different oligomers and different FADD:SA ratios | 77 |
|---|----|

Abstract

This research at UHasselt AFP Group in Diepenbeek, Belgium, focused on Advanced Functional Polymers to tackle the plastic waste problem by upcycling waste polyethylene terephthalate textiles (rPET) with a bio-based soft block. This approach aims to reduce reliance on virgin fossil fuels and minimize waste. The objective was to elongate the soft block to allow a higher weight percentage in the polymer, enhancing its properties and creating extended hard blocks in the final product.

The synthesis of fatty acid dimer diol-succinic acid (FADD-SA) oligomers was optimized using a one-pot melting polymerization technique and analyzed structurally. These oligomers and PET waste were then used in a one-pot condensation polymerization reaction to produce high-value thermoplastic elastomers. The resulting polymer properties were thermally and mechanically characterized to evaluate their product properties.

Optimal oligomer synthesis conditions were 2 hours under an argon atmosphere at 190°C and 3 hours under a vacuum at 220°C with a catalyst. The FADD:SA ratio did not affect oligomer quality but influenced the formation of longer chains. Polymers showed that a higher weight percentage of elongated soft blocks could be added. However, transesterification caused structural randomness, reducing strain at break and maximum stress. This increased soft block content disrupted crystallization, enhancing transparency. The resultant polymers exhibited tacky, glue-like behavior, indicating potential for flexible and reusable adhesive products.

Abstract in Dutch

Dit onderzoek aan de UHasselt AFP Group richtte zich op het aanpakken van het plastic afvalprobleem door afval polyethyleentereftalaat textiel (rPET) te upgraden met een bio-gebaseerde *soft block*, om zo de afhankelijkheid van fossiele brandstoffen te verminderen en afval te minimaliseren. Het doel was om de soft block te verlengen voor een hoger gewichtspercentage in het polymeer, wat zou leiden tot verbeterde eigenschappen en verlengde harde blokken in het eindproduct.

De synthese van vetzuur dimeerdiol-barnsteenzuur (FADD-SA) oligomeren werd geoptimaliseerd via een één-pot smeltpolymerisatietechniek en geanalyseerd. Deze oligomeren werden samen met textiel rPET-afval gebruikt in een één-pot condensatie-polymerisatiereactie om hoogwaardige thermoplastische elastomeren te produceren, die thermisch en mechanisch werden gekarakteriseerd.

De optimale syntheseomstandigheden waren 2 uur onder argon bij 190°C en 3 uur onder vacuüm bij 220°C met een katalysator. De FADD-SA-verhouding beïnvloedde de vorming van langere ketens. Hoewel meer verlengde soft blocks konden worden toegevoegd, veroorzaakte verestering structurele willekeurigheid, wat de breukrek en spanning verminderde. Dit verhoogde soft block-gehalte verbeterde de transparantie. De resulterende polymeren hadden een kleverige consistentie, wat duidt op potentieel voor flexibele, herbruikbare kleefproducten.

1 Introduction

1.1 General introduction

The following sections present an introduction to the research. First, a general overview is given, then the problem statement is discussed, and finally, the research objectives are outlined.

Hasselt University (UHasselt) in Belgium is a dynamic center focused on regional sustainability and innovation through education, research, industry collaboration, and international partnerships [1]. As part of UHasselt, the AFP research group participates in the Sustainable Materials research clusters at the Institute for Materials Research. AFP group focuses on the advanced functionalization of soft polymer materials using controlled polymerization strategies and synthetic technology. The complex polymeric systems have potential in various applications such as adaptive biomaterials, advanced separations, etc. By prioritizing sustainable approaches and responsible resource use.

One of the research lines in AFP Group is based on the upcycling of post-consumer plastics to high-value materials [2]. By researching methods to repurpose plastic waste into advanced materials, and focusing on large-volume waste streams like textiles and packaging. By efficiently transforming these materials, a reduction of virgin fossil-based feedstocks becomes possible and the climate impact of plastic manufacturing can be mitigated. By upcycling postconsumer waste PET it is possible to create thermoplastic copolyesters (TPCs) containing a renewable soft block [3], [4].

1.2 Problem statement

Plastic materials have revolutionized industries and everyday life since Leo Baekeland invented Bakelite in 1907, marking the birth of the modern plastics era. However, plastic production boomed in the post-war period of the 1950s, driven by its versatility, durability, and cost-effectiveness [5], [6]. Fast forward to the present, plastics have become an integral part of our society, and they are used in various applications from packaging and construction to healthcare and electronics. Despite its many benefits, the widespread use of plastic has led to a global pollution crisis. Plastics contaminate our oceans, human and animal health, ecosystems, and climate [6].

The production of plastics relies heavily on fossil fuels, primarily derived from crude oil and natural gas. As a result, the manufacturing process emits substantial greenhouse gases (GHGs) that contribute to climate change [7]. GHGs are emitted at every stage of the plastic lifecycle. Fossil fuel extraction and refining release significant quantities of carbon dioxide (CO₂), methane (CH₄), and nitrous oxide (N₂O) [8]. The manufacturing processes, such as polymerization and extrusion, require energy inputs, usually derived from fossil fuel sources, add further emissions [7]. The chemical processes can emit GHGs as byproducts. Transportation and distribution also contribute GHGs due to fossil fuel-powered vehicles. In waste management, landfilling releases methane, and incineration emits CO₂ and other pollutants. These processes collectively increase GHG emissions, worsening the greenhouse effect [7].

Moreover, plastic production generates vast amounts of waste, with a significant portion ending up in the environment due to inadequate waste management systems and improper disposal practices. Plastic production has increased further and globally, 400.3 million metric tons were produced in the year 2022 worldwide [9]. According to the Organization for Economic Co-operation and Development (OECD) only 9% of the plastics were successfully recycled in 2022, meaning most of the materials are mismanaged, uncollected, landfilled, or incinerated [10]. The OECD organization assembled a first Global Plastics Outlook Database concerning the share of plastics treated by waste management category, after disposal of recycling residues and collected collected litter in 2019 [10]. The estimated percentages by category are represented in Figure 1, parted by region.

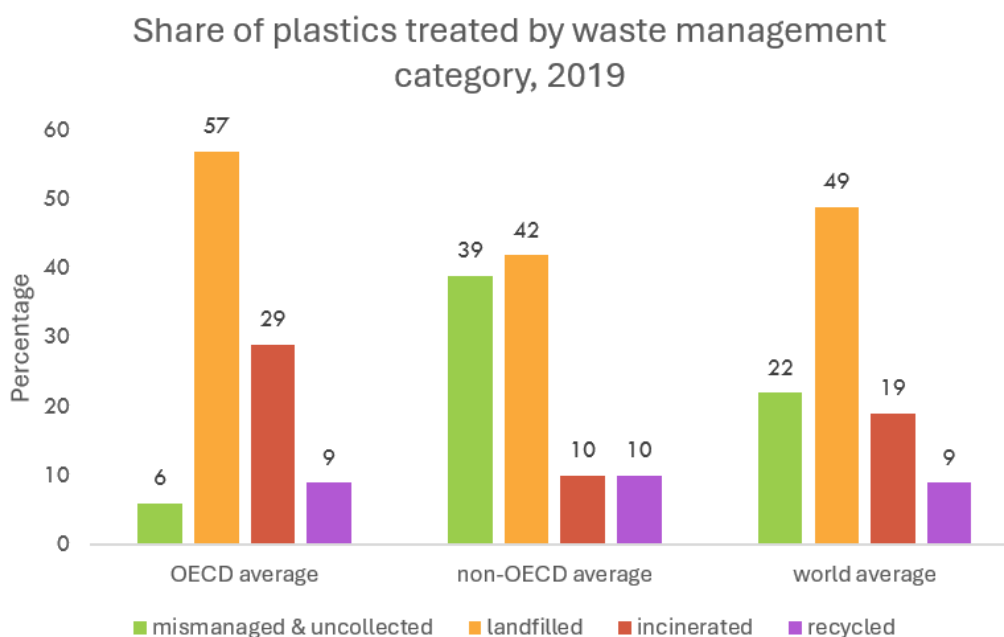


Figure 1: Share of plastics treated by waste management category, after disposal of recycling residues and collected litter in 2019. Modified from [10].

Traditional fossil-fuel-based plastics are not biodegradable, however sunlight can weaken and break them down into microplastics [6]. These microplastics, found in both aquatic and terrestrial ecosystems, can be ingested by organisms, leading to potential health issues and environmental impacts [11], [12]. Microplastics can adsorb toxic chemicals, disrupt soil health, and affect biodiversity [5, 6], [11], [13].

In light of these challenges, there is a growing urgency to address plastic pollution through innovative solutions, including waste reduction, recycling technologies, and the development of biodegradable alternatives. Within the AFP group they conduct many different research lines, that fit into this idea of sustainable alternatives and techniques. They were already able to upcycle PET waste in a one-pot synthesis process to thermoplastic elastomers. Biobased fatty acids were used as a soft block segment in the TPCs created [3], [4]. Besides the synthesis with fatty acids to TPCs, it was found that the PET repeating units in the same synthesis process can be converted to polybutylene terephthalate (PBT) repeating units by addition of biobased 1,4-butanediol instead of ethylene glycol [4]. In this study a 60 wt% of soft block was found to be the maximum limit while maintaining decent mechanical properties for the TPCs, as they become more and more viscous when more soft block is added. This limitation makes it more difficult to synthesize soft, sustainable elastomers using this method [3], [4].

In the year 2021 over 55 million tons or 25.47 million metric tons of polyethylene terephthalate (PET) was produced, making it a high-volume produced plastic, schematically represented in Figure 2 [9], [14], [15], [16]. This and the availability, makes PET an excellent candidate for the upcycle projects AFP group focuses on.

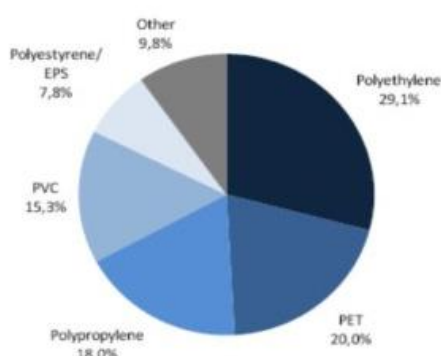


Figure 2: World thermoplastic resin capacity in the year 2008 [17].

1.3 Research goals

The primary aim of this research project is to synthesize longer soft blocks to ultimately create longer hard blocks in the final polymer structure. Achieving this goal involves several key objectives, each focusing on different aspects of polymer synthesis, optimization, and characterization.

The first objective is the synthesis of FADD-SA oligomers. These oligomers serve as the soft blocks in the polymer chain, and their length and structural integrity are crucial for the desired properties of the final polymer. The synthesis process involves precise control over the reaction conditions to ensure the production of oligomers with consistent and optimal characteristics. To optimize the synthesis process different parameters are adjusted such as temperature, catalysts, and reaction times.

Characterization techniques, such as nuclear magnetic resonance (NMR) spectroscopy, and gel permeation chromatography (GPC), will be employed to analyze the molecular structure and molecular weight distribution of the synthesized oligomers.

The second objective focuses on incorporating polyethylene terephthalate (PET) upcycling methods to synthesize thermoplastic copolymers (TPCs). By integrating PET upcycling techniques, this research aims to create high-value materials from PET waste, contributing to sustainable practices in polymer science.

In this process, the FADD-SA oligomers will react with PET, forming the backbone of the TPCs. The synthesis of TPCs is carefully monitored to ensure efficient incorporation of PET into the polymer matrix, maintaining the desired balance between soft and hard blocks. The resulting TPCs can be characterized using the same techniques as for oligomer structure characterization.

The final objective involves the mechanical and thermal characterization of the synthesized polymers. This step is crucial to understand the relationship between the polymer's molecular structure and its macroscopic properties. The mechanical properties, such as tensile strength, elasticity, and toughness, are assessed using tensile testing analysis. The thermal properties, including melting temperature, are determined using differential scanning calorimetry (DSC).

1.4 Master's thesis content

This thesis is structured to guide through the research on the synthetization of longer soft blocks for enhanced hard blocks in polymers. It includes five main chapters and an appendix.

Chapter 1 provides a general introduction, presenting the research's significance, outlining the problem statement, and detailing the research goals. It concludes with an overview of the thesis structure.

Chapter 2 reviews the relevant literature, focusing on PET recycling methods and biobased thermoplastic elastomers. It also summarizes previous research findings, highlighting gaps and opportunities for further study.

Chapter 3 describes the materials and methods used in the research. It details the synthesis of FADD:SA oligomers, the incorporation of PET upcycling techniques, and the characterization processes. Each method is explained to ensure reproducibility and clarity.

Chapter 4 presents and discusses the research results. It systematically organizes the findings from synthesis, optimization, and characterization. It compares these results with existing literature, discussing their implications and addressing any differences.

Chapter 5 concludes the thesis by summarizing the key findings and their significance. It reflects on the achievement of the research goals, discusses broader implications, and suggests future research directions.

The appendix part includes supplementary tables and figures with additional data referenced throughout the thesis. These materials provide further insights and detailed information supporting the main text.

2 Literature study

2.1 Recycling of polyethylene terephthalate

2.1.1 Polyethylene terephthalate (PET)

PET is a thermoplastic polymer derived from petroleum-based chemicals commonly used in textile and packaging industries due to its strong, clear, and lightweight characteristics. Most PET is used for polyester fiber production (60%), followed by the bottle industry (30-40%) [18], [19]. While recycling has improved over the last decade, there is still a long way to go, especially when it comes to recycling PET fibers from textiles, as it forms more than half of the total fiber volume [19]. Due to limited reuse and recycling capabilities in Europe, a significant portion of discarded and donated clothing and other textile items are exported to other continents, such as Africa and Asia, where they most likely end up in landfills [20]. Yuan et al. stated that every minute, more than one million PET plastic bottles are globally sold, over 90% of them are discarded into landfills or the ocean, and at least 450 years are necessary for plastic bottles to degrade completely [21]. Due to the widespread utilization of PET fibers in textiles and the common use of plastic bottles, the PET waste stream has become voluminous, posing a significant environmental challenge. The high-volume production and consumption contribute to the accumulation of waste in landfills, oceans, and natural habitats. Effective waste management strategies and sustainable alternatives are essential to mitigate the adverse impacts of PET plastic waste on ecosystems and human health.

Chemical background

Chemically, PET is a polyester composed of repeating units of ethylene glycol and terephthalic acid, giving it a linear, semi-crystalline structure, represented in Figure 3. The ring structure gives the polymer more stiffness, while the ethene group gives a more flexible characteristic. This arrangement contributes to its excellent mechanical properties, including high tensile strength, stiffness, and dimensional stability. PET exhibits good chemical resistance, making it suitable for food contact materials within the packaging industry. Additionally, PET is lightweight and transparent, making it more versatile for various uses [16]. PET is widely used for its balanced properties, however there are some limitations that affect its suitability for certain applications. The thermal properties of PET can limit its use and processing options. For example, PET has a glass transition temperature (T_g) of approximately 70-80°C transferring from a hard, glassy state to a more rubbery state, and a melting temperature (T_m) of 250-260°C, where the PET material transitions from a crystalline or semi-crystalline solid into a molten liquid. The crystallization temperature (T_c) ranges from 110-140 °C, where the material can crystallize from the molten state upon cooling [22], [23]. The crystallization process of PET is complex due to various factors besides temperature and molecular weight that have significant influence. The moderate crystallization rate, sensitivity to cooling rate, and impact of nucleating agents make PET distinct from other polymers. These factors must be controlled carefully to achieve the desired properties of PET [24].

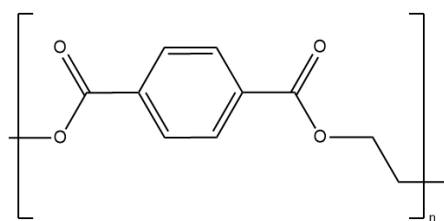


Figure 3: Structure of PET repeating unit

Production of PET

PET is generally produced by esterifying terephthalic acid (TPA) with ethylene glycol (EG) or by esterifying dimethyl terephthalate (DMT) with EG. First, an intermediate monomer bis(2-hydroxyethyl terephthalate) (BHET) is formed, releasing either water or methanol, followed by polycondensation of BHET to form PET in the melt phase while releasing EG [25]. The synthesis reactions are represented in Figure 4.

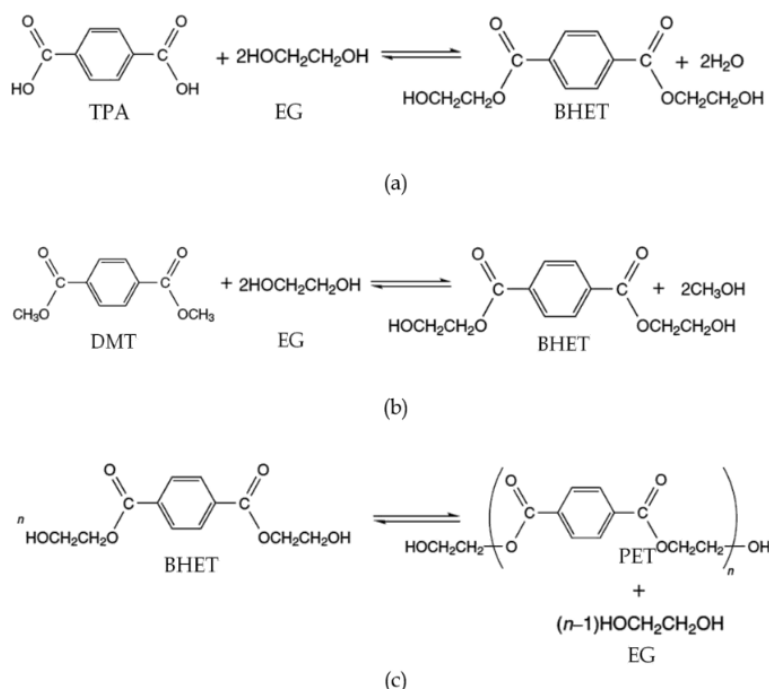


Figure 4: Reaction scheme for the synthesis of PET. BHET formed by TPA and EG (a), or DMT and EG (b), and polymerized to PET (c) ([25], [24], p. 66).

Within the production process of PET, it is important to control the molecular weight synthesized. The molecular weight refers to the average mass of the polymer chains, usually expressed in number-average molecular weight (M_n) and weight-average molecular (M_w). A typical molecular weight for the polymer lies between 8 000- 50 000 kg/mol [26], [27]. Creating polymers with a high molecular weight, comes with several challenges such as the process conditions, the prevention of degradation and the control of the polymerization process. Carefully managing factors such as using high-purity materials, constant water removal, appropriate catalysts, reaction conditions, the minimization of degradation and real-time monitoring, are crucial for producing high molecular weight PET. The polydispersity is the ratio of M_w to M_n , indicating the distribution of molecular weights. A typical polydispersity value for industrial produced PET is around 2 [28].

As PET is such a widely used material, different grades are conducted with specific characteristics. First, there is film grade PET, which excels in flexibility, moisture resistance and ability to produce a thin layer. This grade is mostly used in food packaging, but also screen protectors for mobile phones and electronics. Secondly, the bottle grade PET is probably the most known. It is used in beverage bottles and jars, due to its strength and clarity. Lastly, there is textile grade PET, used in clothing and home furnishings. Textile grade PET can be spun in durable, wrinkle-resistant fabrics with different characteristics [29]. Some well known companies that manufacture PET on a large scale are Indorama Ventures, SABIC, Alpek, and novapet [30], [31].

2.1.2 Recycling and waste management

Primary recycling

Primary recycling is the direct reuse of clean, discarded polymer materials to make new products while retaining their original properties. Often carried out by manufacturers as a closed-loop process for post-industrial waste [32]. While post-consumer waste can also undergo primary recycling, challenges such as selective collection and manual sorting increase costs and limit its popularity among recyclers. Before reintegration, the material undergoes grinding processes to enhance homogeneity and facilitate blending with additives and other polymers. Subsequently, melting and shaping methods, such as injection molding and extrusion, are employed, which are primarily suitable for thermoplastic polymers, including PP, PE, PET, and PVC. Closed-loop recycling ensures efficient material reintegration into the production cycle, with impurities removed, stability maintained for high-temperature processes, and materials processed similarly to virgin ones. It should be noted that only thermoplastic homopolymers can be recycled using this technique [33].

Secondary, or mechanical recycling

Mechanical recycling is a process whereby plastic waste is reclaimed and converted into new products through a series of physical processes. The process starts with collecting and sorting post-consumer materials, based on their color and resin type [34]. Once sorted, the plastic waste is cleaned to remove contaminants such as food, impurities, and other plastics [35]. Subsequent to sorting, the plastic waste is shredded into smaller pieces and washed at a higher temperature for a short time to remove labels, glue, and dirt. The cleaned chips are then melted and extruded into small pellets [35]. The greater complexity of the waste stream differentiates it from primary recycling, where the cleaning steps of the process are unnecessary [36]. Furthermore, secondary recycling typically results in a lower-quality product compared to primary recycling due to the potential degradation of polymer properties during previous use and processing cycles. As a result, the applications for secondary recycled materials are often limited, and the economic viability of the process may be compromised [36], [37].

Tertiary, or chemical recycling

Unlike mechanical recycling, which involves melting and reshaping, chemical recycling breaks down the plastic into monomers or other useful chemical compounds that can be used as feedstock for new materials [38]. While this process sounds promising for mixed or contaminated plastics, it still faces several challenges. One major issue is the complexity and costliness of chemical processes required for depolymerization and purification. Scaling up these technologies to handle large volumes of plastic waste remains a challenge, as well as raising concerns about the environmental impact of chemical recycling processes, such as energy consumption, emissions, and hazardous by-products [39], [40].

Quaternary recycling

Quaternary recycling is divided into incineration and landfill.

Incineration and landfilling are two common methods of disposing of plastic waste, but they come with significant environmental challenges. Incineration involves burning plastic waste at high temperatures to generate heat and electricity. While this method can reduce the volume of waste and recover energy, it also releases harmful pollutants, including GHGs, dioxins, and other toxic substances, into the atmosphere. All this contributes to air pollution and climate change, posing a risk to human health and the environment [17].

Landfilling, on the other hand, involves burying plastic waste in landfills, where it can take hundreds to thousands of years to decompose. Plastic materials do not readily biodegrade, so they persist in landfills, taking up valuable space and potentially leaching harmful chemicals into the soil and groundwater. Moreover, as plastics degrade, they can release methane, contributing to global warming. Both options contribute to the problem of plastic pollution, as they fail to address the underlying issues of overconsumption and unsustainable production and disposal practices [41].

Problems with recycling nowadays

As discussed before, many problems still occur with any recycling method. Mechanical and chemical recycling methods pose issues. For example, mechanical recycling can result in poor quality materials due to the mixing of different, immiscible materials, and contaminants when separation is adequate [[42], [43]. In the case of chemical recycling, the use of harsh chemicals creates an unsustainable process for the environment. Air pollution, the release of toxic gases, and high energy consumption are common problems with incineration. The recycling methods and problems are shown in Figure 5. As can be seen, the chemical recycling method provides the most promising route for PET materials when the use of harsh chemicals and energy consumption can be limited. In Western Europe, plastic waste generation has grown by about 3 % annually, while mechanical recycling has increased by 7 % per year. In 2003, only 13.1 % of plastic waste was mechanically recycled, 1.7 % was chemically recycled, and 22.5 % was used for energy recovery [44]. Although this data is older, Plastics Europe [45] confirms that mechanical recycling is still the main method used, but not all plastics are recycled, with most plastic incinerated [10], [46]. In 2020, post-consumer plastic waste sent to recycling reached 35% across Europe, as shown in Figure 6 [46].

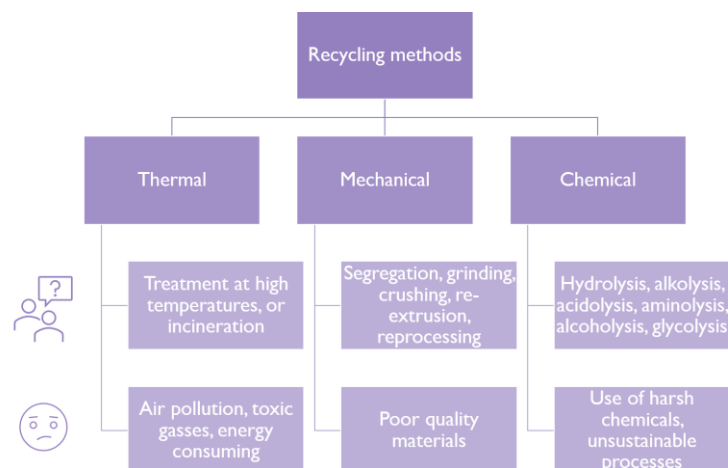


Figure 5: Schematic overview of the different recycling pathways and their predominant problems, modified from [40].

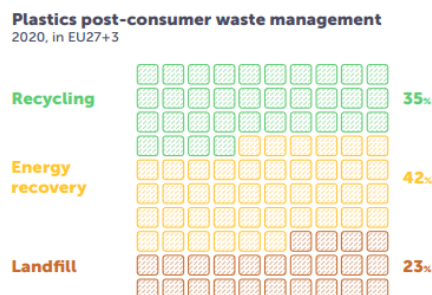


Figure 6: Schematic overview of the plastic post-consumer waste management in 2020 in EU27+3 [39], p. 27)

When it comes to PET collection rates in Europe, Belgium is in the top three with a collection rate of 92 %, with only Denmark (96 %) and Germany (95 %) scoring higher [47]. On average PET beverage bottles have a recycling content of 24% in Europe in the year 2022. Most European countries have established or are going to establish by 2025 a deposit return system (DRS) to increase collection volumes of PET bottles. In 2022 on average 75% of collected PET bottles were recycled [48]. However the great efforts on the collecting and recycling of PET bottles, a decent recycling value chain for PET textiles is still missing. When textiles claim they are made from recycled materials, it is mostly consistent of recycled PET bottles, downgrading the valuable recycle [49].

2.1.3 Depolymerization of PET

One way of using chemical recycling is the depolymerization of PET. Depending on the used solvent, There are many ways to depolymerize PET material. A few examples of the chemical recycling ways of PET are hydrolysis, acidolysis, alkalolysis, aminolysis, alcoholysis, and glycolysis [50].

Hydrolysis

Hydrolysis uses water to break the bonds within the material. Hydrolysis in a neutral environment, using solely water to break PET bonds through a self-accelerating process, may experience a slight rate increase with the addition of a salt catalyst. The addition of an acid (nitric acid or sulfuric acid) or a strong base (hydroxide ions), further improves the rate of the hydrolysis process [51]. The hydrolysis process typically occurs with higher temperatures around 200-300°C and a pressure of 1-4 MPa [51]. Neutral hydrolysis could be an interesting depolymerization method if the rate would be more sufficient. The addition of strong acids and bases makes the process less sustainable.

Alkolysis and acidolysis

Alkolysis and acidolysis, are reactions similar to hydrolysis, in which the base or acid breaks down the bonds. Acidolysis can be used along with a heating system without solvent or catalyst to break down PET materials [52]. To prevent loss of the acid used, the heating system was switched on and off. Finally, various oligomers and monomers were identified, which were then used in curing reactions to result in adducts with different properties [52]. The use of harsh chemicals such as a strong base or acids, takes of the environmental aspect of the depolymerization.

Aminolysis

PET fibers can be depolymerized through aminolysis using ethanolamine and chemicals such as glacial acetic acid, sodium acetate, and potassium sulfate as catalysts. This depolymerization process can achieve a high yield and purity of bis(2-hydroxy ethylene)terephthalamide (BHETA) within a shorter reaction time [53]. This method is less known than others and still needs to be explored further.

Alcoholysis

The deconstruction of PET can be done by alcoholysis, in which an alcohol group from an ester is replaced by another alcohol in a process similar to hydrolysis [54]. Typically, methanol or ethanol is used for this process. Methanol along with a raised temperature of 180-280°C and a pressure of 20-40 atm, will break down the PET into the dimethyl terephthalate (DMT) and ethylene glycol. The obtained DMT is identical to that of virgin DMT and the EG can be recovered easily. On the downside, the reaction procedure is costly and therefore used less [55].

Glycolysis

The last method to depolymerize PET materials is glycolysis. By using glycols such as Ethylene Glycol (EG), PET can experience a trans-esterification reaction where ester linkages can be broken down and replaced with hydroxyl terminals to form molecules including BHET [56]. Glycolysis uses fewer resources and operates at lower temperatures and pressures than other methods like methanolysis. It also does not pose challenges such as corrosion and waste management such as acidolysis and alkalolysis, making glycolysis a widely used method. The optimal parameters for the glycolysis of PET and different types of rPET were investigated by Aguado, A. et al. [57]. The best reaction conditions, and a ZnAc₂-catalyst achieved yields ranging from 76,93% to 86.82% depending on the type of PET used. With these conditions, and using distillation, up to 70% of EG was able to be recovered, making it an economical and environmentally valuable way to recycle PET waste materials chemically [57].

Overview

The different depolymerization reactions of rPET are shown in Figure 7.

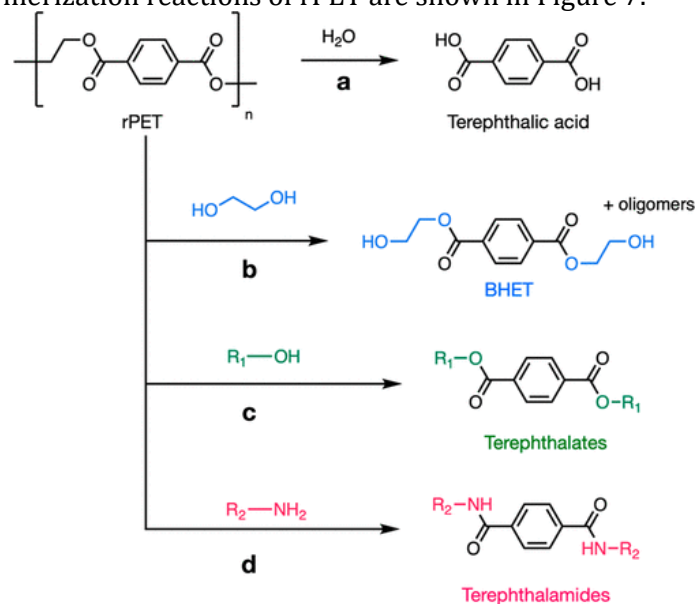


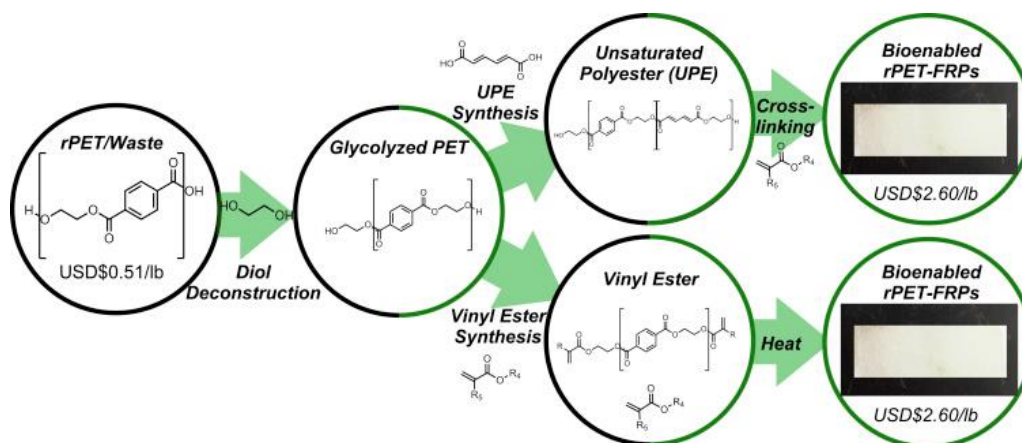
Figure 7: Diverse depolymerization/upcycling strategies for rPET, using (a) hydrolysis, (b) glycolysis, (c) alcoholysis, and (d) aminolysis [58], p. 1749

2.1.4 Upcycling

An alternative approach to managing plastic waste material is the concept of ‘upcycling’. Upcycling differs from recycling in that it does not break the material into new materials but transforms them into something better instead [59]. The upcycling of materials is becoming more popular in today’s society and can be done as simple DIY projects at home with household waste, to scientific upcycling to try to achieve a circular economy and reduce the usage of virgin materials. For example, the chemical upcycling of plastics breaks them down into smaller components or monomers and reassembles them into high-value materials by using chemical processes such as depolymerization.

One way of upcycling rPET into polyurethane acrylate (PUA) by bio-based glycolysis with cardanol diol, followed by repolymerization to form PUA coating that is UV-curable [60]. The process is monitored by using NMR spectroscopy. The researchers concluded that a total depolymerization of PET can be achieved within 90 minutes while using tetrabutyl titanate as a catalyst at 230 °C. The formation of PUA was confirmed by 1H-NMR tests where the bonds were visual [60].

Another research states that rPET can be deconstructed using transesterification with a diol from biomass along with a catalyst such as titanium butoxide [61]. Increasing the amount of the diol (either ethylene glycol or 1,4-butanediol) led to a decrease in the molecular weight of rPET. An excess amount of diol makes sure that the rPET ends with hydroxyl groups, which makes it easier to work with. The deconstructed rPET can then be synthesized into unsaturated polyester (UPE) by adding bio-derivable olefinic acid in a melt blending process with a transesterification catalyst. By crosslinking the UPE, bio-enabled rPET- fiberglass reinforced plastics (FRPs) can be created. The deconstructed rPET can also follow a vinyl ester synthesis and heat treatment to synthesize the rPET-FRPs. Vinyl ester synthesis involves a chemical process where the ester groups of rPET are modified to create vinyl esters. The overview of the synthesis of rPET-FRPs is represented in Figure 8 [61].



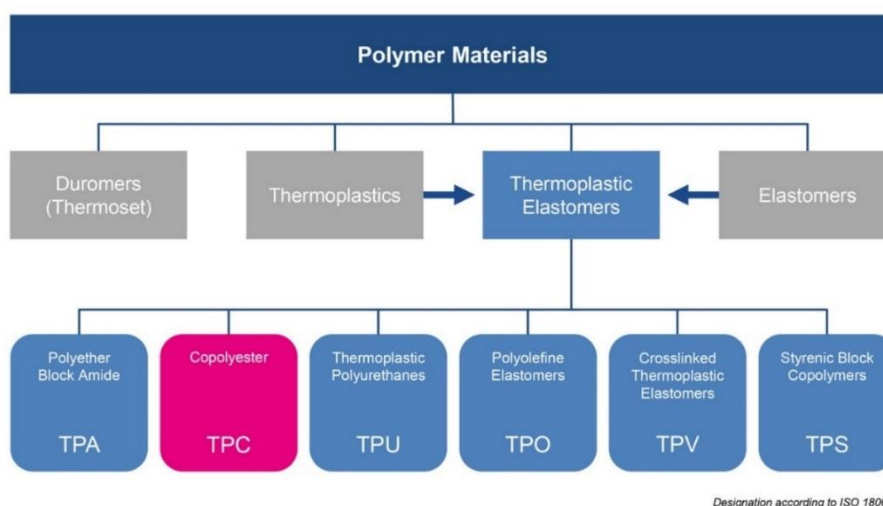
Prices as of August 2018

Figure 8: Overview of rPET converted to higher-value FRPs through two different routes ([61], p. 1008)

Post-consumer plastics can be used to upcycle to new biodegradable plastics. First, by breaking down PET into its basic building blocks using an enzyme (a thermostable polyester hydrolase). Followed by a reaction with bacteria, *Pseudomonas umsongensis* GO16, that will eat the building blocks and produces PHA bioplastic. These bacteria can be modified to produce another material called hydroxyalkanoxy-alkanoates (HAAs), which can be used to make bio-PU through a chemical process. This way it is possible to create more valuable materials, while keeping an eye on green environmental technologies [62].

2.2 Thermoplastic elastomers

Thermoplastic copolyesters (TPCs), or thermoplastic polyester elastomers (TPEEs) are a class of thermoplastic elastomers (TPEs), that are materials that exhibit both thermoplastic and elastomeric characteristics [63], as shown in Figure 9. Thermoplastics are polymers that become soft and moldable at a certain temperature and harden to that shape when cooled, which means that they can be processed repeatedly. Elastomeric properties in a polymer can be shown as viscoelastic behavior. The combination of both properties can be used as an advantage such as longer usage and better mechanical properties all within a larger temperature range [64]. Copolyesters are polyesters that contain different repeating monomers instead of one monomer. Thermoplastic copolyesters are mostly used in engineering plastic applications such as automotive, adhesive, and industrial applications [65], [66]. The global production of TPC products in 2022 is estimated around 345 kilo tons [66]. Block copolymers only qualify as a TPE if they include a soft material as one of its blocks (ex. Polydiene, siloxane, polyether), which necessitates the need for a more sustainable approach [67]. Adding a biologically sourced component to achieve these engineering plastics, improves the environmental impact and reduces the usage of virgin feedstock materials.



Designation according to ISO 18064

Figure 9: Categories of polymer materials [68]

Since most of the TPEEs are petroleum-based, they are considered unsustainable. By replacing the hard and/or soft segment with a biobased substitute, biomass-derived and sustainable TPEEs are possible.

2.2.1 Sustainable hard segment

The first option is to change the hard segment to a more eco-friendly one. A few alternatives for PET have emerged, such as poly(butylene succinate), and to some extent poly(lactic acid) (PLA). (PBS) [69]. Another option is to replace the fossil-fuel-based terephthalic acid (TPA) which is used for PET and PBT production, with a sustainable variant such as (2,5-furandicarboxylic acid) (FDCA) [70]. The bio-based monomer makes it possible to create new polyesters, such as poly(ethylene 2,5-furandicarboxylate) (PEF) and poly(butylene 2,5-furandicarboxylate) (PBF) [70], [71], [72].

Lastly, it is also possible to substitute PET with bio-PET or rPET. Bio-PET is a bio-based alternative to PET but derived from sugar cane instead of fossil fuel [73]. rPET is another valuable way of decreasing the GHGs compared to virgin PET. Butanediol (BDO) can break down the PET to create polybutylene terephthalate (PBT). When polytetrahydrofuran (PTHF), is added to the mixture, PBT-PTHF block copolymers can be synthesized, as shown in Figure 10 [74]. When the length of the hard block increases, the melting temperature rises and becomes comparable to that of pure PBT. The potential usage of low-value rPET monomers in engineering TPE development seems possible when the residues on block length are taken into caution [74].

Another sustainable soft block is a hydrophobic fatty acid dimer diol (FADD). Copolyesters can be made using a solid-state modification process on PBT and FADD [76]. By varying the block length and composition of the copolyester, the properties can be tailored. Researchers found that there is a dependence of the chemical microstructure and morphology on the FADD content in the copolyesters. Microphase separation in block copolymers, such as PBT/FADD copolyesters, involves the self-organization of distinct polymer blocks into nanometer-sized domains due to their chemical incompatibility. This separation begins when FADD content exceeds 10 wt% and becomes more pronounced when the content further increases. At 41 wt%, an extensive phase separation occurs, disrupting the crystalline lamellar stacks and introducing a finer structure in the amorphous regions. These regions significantly influence the polymer's thermal and mechanical properties, making them crucial in understanding the material's behavior and performance [76].

The FADD can be used to upcycle rPET, as described by A. Karanastasis, et al.[4]. Here post-consumer PET bottles are used as a hard block to create a high-performance TPC, following the reaction mechanism shown in Figure 12. FADD is selected as a soft block for its hydrophobicity and controlled functionality, ensuring compatibility and avoiding excessive branching during polymerization. This bio-based fatty acid dimer diol can be derived from linoleic acid, which can be found in sunflowers and safflowers [3]. With an average molar mass of ~550 g/mol, FADD blends effectively with high molar mass rPET. It experiences transesterification to promote extensive chain scission in rPET, by breaking down long polymer chains into smaller segments, which is crucial for forming segmented copolymers with tailored properties [4].

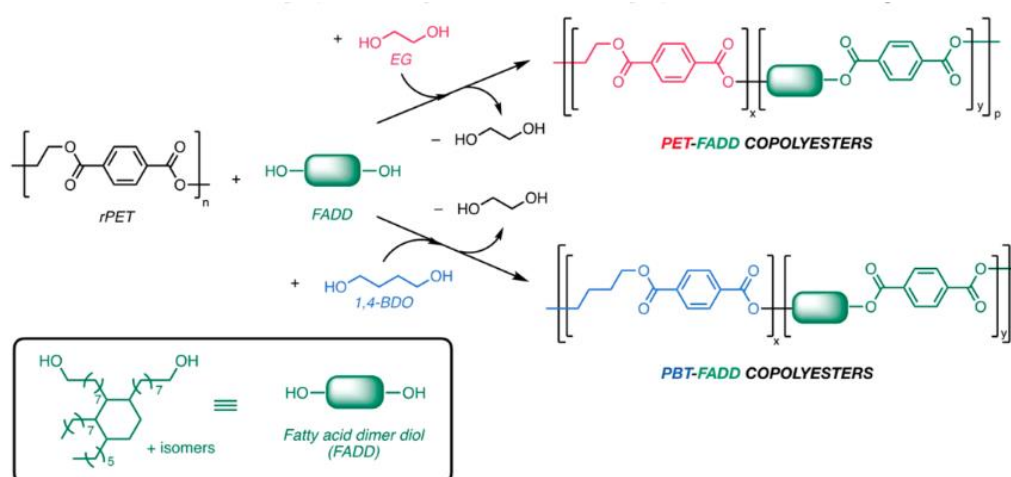


Figure 12: The Complementary synthetic pathways to high-performance TPCs by combining rPET with FADD ([4], p. 352)

The TPCs were synthesized using a one-pot melt polycondensation process [4]. The first series used rPET, FADD, excess EG, and titanium tetrabutoxide (TBT) to achieve optimal segment distribution. The second series replaced EG with excess 1,4-butanediol (BDO), forming PBT units. EG accelerates PET depolymerization, forming essential hydroxyl end-groups, but without EG, transesterification is slow due to high FADD molar mass. High melt polycondensation temperatures (~250°C) cause polymer degradation and chain elongation competition. Increasing temperature and applying a low vacuum after initial depolymerization recover EG and increase polymer molar mass [4]. In this research a maximum wt% of soft block was estimated at 60 wt%, due to the increasing viscosity. The introduction of a longer soft block, or extending the FADD by reaction, may cause the wt% to go up since the hard block will lengthen as well, note that the soft block and hard block stay miscible as the wt% and molecular mass of the soft block increases.

2.2.3 Elongated soft segment

The molar mass of the soft block determines the property limits of the mixture, with higher molecular weight causing phase separation over a broader range of compositions. This can be explained by the Flory-Huggins theory that helps predict whether a polymer mixture will be homogeneous or phase-separated [77], [78]. A Flory-Huggins phase diagram for a 2-component polymer blend is given at a fixed temperature in Figure 13.

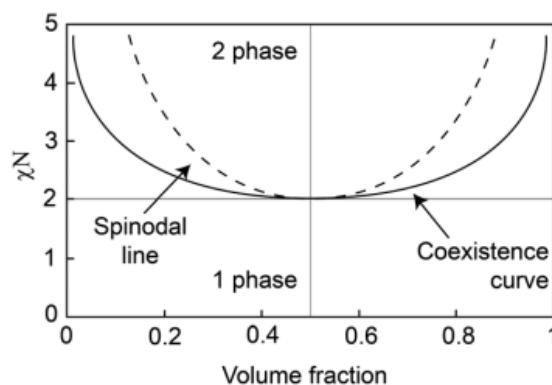


Figure 13: Flory-Huggins phase diagram for components with equal degrees of polymerization [71]

On the X-axis, the volume fraction is displayed, which is a measure of the proportion of a component in a mixture based on its volume. This can be changed for weight percent (wt%) as it does the same, but based on its mass instead of volume. On the Y-axis the Flory-Huggins interaction parameter (χ) is displayed, which is influenced by the molecular weight (M_n) of a polymer. A higher M_n , means the number of segments in the polymer chain also increases and affects the interactions between polymers as displayed by χ [79]. It is possible to create a similar graph where the X-axis is displayed as the wt% of a first component, the soft block for example. And the Y-axis is displayed as the molecular weight of the same component. A longer soft block will decrease the compatibility and lower the curve, as seen in Figure 14 [79-81]. When synthesizing polymers, it is important to have the miscibility in mind as it can affect the polymers performance. A longer soft block can cause phase separation when added in the same wt% as a shorter soft block.

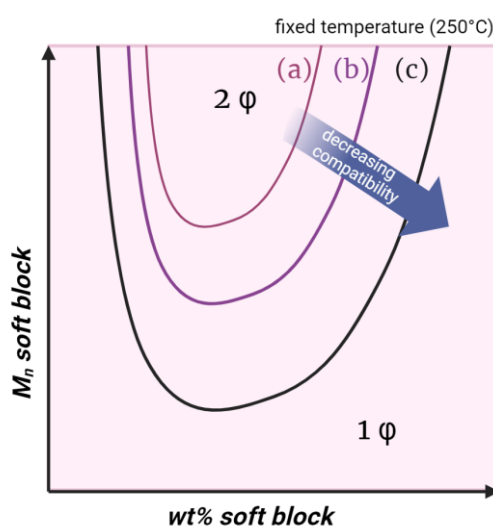


Figure 14: Property boundaries set by different soft block (a, b, and c) molar mass, made with biorender.com

Besides the miscibility, is the composition of the polymer material also dependent on the molecular weight of the polymer, as schematically shown in Figure 15. A longer soft block will increase the length of the equivalent hard block as well, bettering the structural properties of the polymer. Even though the chemical composition, meaning the type and ratios of monomers/oligomers, are the same, changes in block length within the copolyester can alter its properties [82], [83]. When working with a waste stream of rPET, it is recommended to adjust the block length of the soft segment. This way, the equivalent hard block also increases in length, when a fixed wt% is used for the soft block.

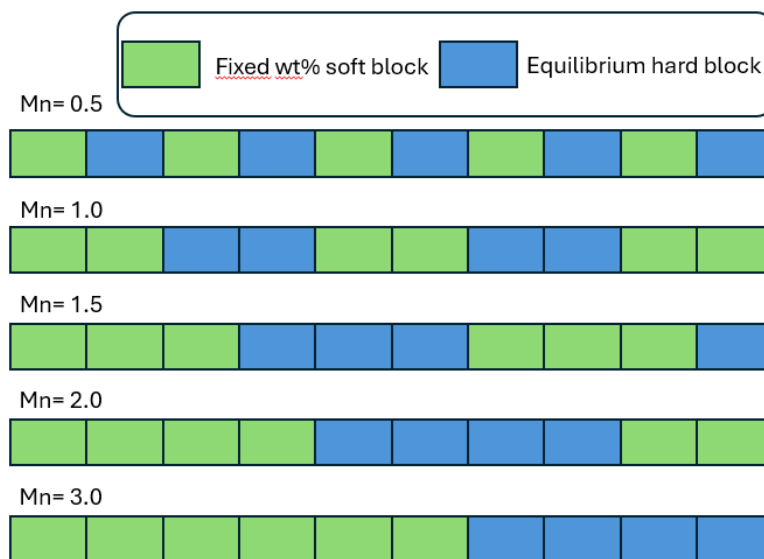


Figure 15: Schematic representation of distribution between a fixed wt% soft block and different length of hard block (modified from [84], p. 606)

Keeping these two concepts in mind, the influence of the block length on the properties can be studied in more detail. The next paragraphs will give some case studies in which the soft block length is modified, followed by an overview of the changes.

Fakirov S. et al., synthesized a series of poly(ether/ester) copolymers by combining poly(butylene terephthalate) (PBT) as a hard segment, and poly(ethylene glycol) (PEG) as a soft segment [84, 85]. The reaction mechanism is shown in Figure 16. The copolymers display a three-phase morphology with an amorphous phase for each segment and one crystalline phase for the PBT segment. The longer the PBT blocks, the higher the glass transition temperature (T_g) and the higher the melting temperature (T_m). The tensile strength and modulus increase when the PBT block is longer, and the flexibility reduces. The longer PEG blocks, T_g decreases and maintains T_m , while the elasticity, impact resistance, and flexibility are enhanced [84, 85].

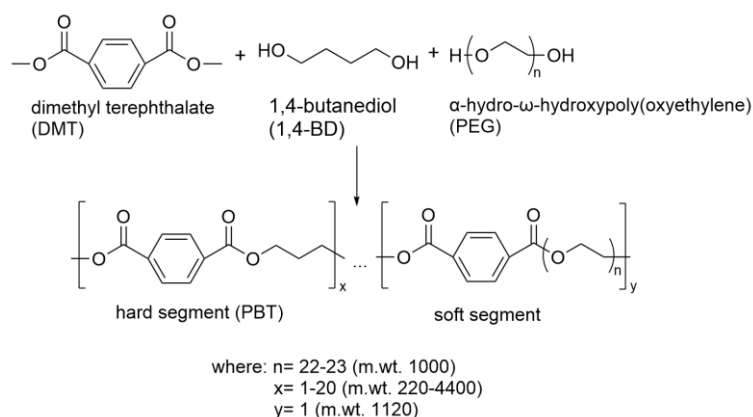


Figure 16: Reaction mechanism for the synthesis of PBT/PEG block copolymer(modified from: [84], p. 605).

Another study focuses on the synthesis of segmented block copolymers based on dimerized fatty acids and poly(butylene terephthalate) (PBT) [86]. In the case of mechanical properties, alter the compatibility of the polymer without significantly affecting the storage modulus or crystallization enthalpy. Longer fatty acid blocks reduce the compatibility between PBT and the amorphous phase, increasing the average length of PBT segments. This leads to the potential formation of an extra amorphous phase with higher PBT concentration, affecting the thermal properties. A higher wt% of the PBT fraction increases the T_g and T_m of the polymer. When the molecular mass of the fatty acid increases, the T_g decreases and T_m increases [86]

Cella, R. J. researched the morphology and physical properties of copolyester thermoplastic elastomers [87]. The elastomers were synthesized by a transesterification reaction of dimethyl terephthalate with 1,4-butanediol (4G), dimethyl terephthalate (DMT), and poly(tetramethylene ether) glycol (PTMEG) as segments for the backbone of the polymer, as shown in Figure 17.

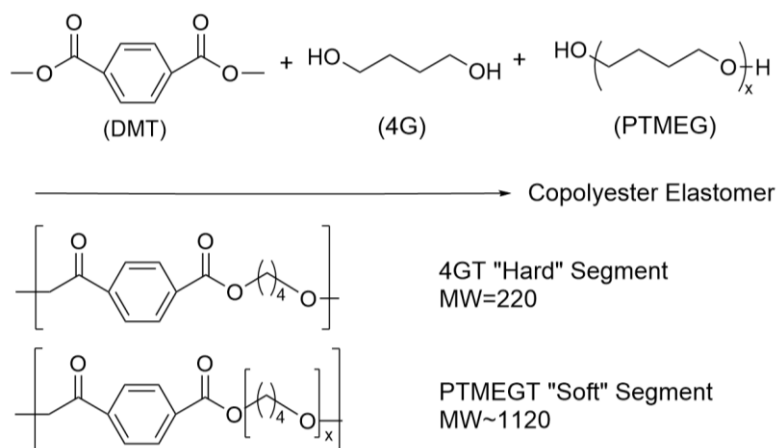


Figure 17: Synthesis of TPC from DMT, 4G, and PTMEG (modified from: [87], p. 729).

PTMEGT is the amorphous, soft segment, which contributes to the elasticity of the material. 4GT is the crystalline, hard segment, which gives the polymer its strength and thermal stability. The study concludes that the block length, particularly the balance between 4GT and PTMEGT segments, influence the thermal and mechanical properties. The increase in T_g with higher hard segment content suggests incomplete phase separation, with some hard segments dispersed in the elastomeric phase. Short 4GT segments do not crystallize, and longer ones are hindered by chain entanglements and high melt viscosity. Higher hard segment content also raises pseudo-crosslinking, contributing to the T_g increase. The T_m rises with increasing 4GT content, nearing to 230°C as the 4GT fraction approaches 100 wt%. This is due to longer crystallizable blocks. T_m asymptotically approaches the melting point as the average hard block length increases. The

tensile behavior is given in Figure 18. The polymers exhibit three distinct regions, with higher crystalline content leading to more pronounced yield points and earlier breaks. The first region is the initial deformation, characterized by high initial modulus. The second region is the draw plateau and the third is the elastomeric behavior. An increase of 4GT content, increases the Young's modulus and yield stress as the stress required to deform the crystalline matrix and the force required to orient the crystallites both rise as the amount of crystallizable material increases [87].

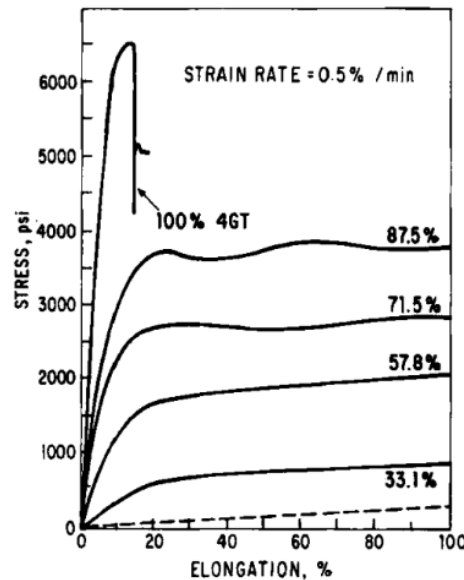


Figure 18: Stress-strain curves of TPC as a function of the 4GT content ([87]p. 739)

Y. Xu et al. (2023), described the block length is significant for the phase separation, mechanical properties, thermal properties, processing, and miscibility [65]. As for mechanical properties, a longer hard block contributes to a higher tensile strength due to its ability to form crystalline regions or strong physical cross-links between the polymer chains. A shorter soft block, increases the polymer's flexibility and toughness, as they allow more movement and entanglement of polymer chains in the amorphous regions, which enhances the impact resistance and elongation at break. The thermal properties are altered, as the length of both soft and hard block influences the glass transition temperature (T_g). The T_g corresponds to the transition from a glassy to rubbery state of the polymer. Longer hard blocks can increase the T_g of the crystalline phase, while shorter soft blocks decrease the T_g of the amorphous phase. When increasing the block length, researchers found that the longer, the more compatible they are, and therefore improve the overall material homogeneity[83].

A longer soft block can be synthesized by an esterification reaction between a diol and an acid like succinic acid, followed by a polycondensation reaction. Poly(1,4-butylene/2,3-butylene succinate) (PBBS) is a biobased oligomer, from succinic acid (SA) and 1,4 butanediol (1,4-BDO), that can be used to synthesize PBT-PBBS copolyesters as shown in Figure 19. The synthesis of the oligomer is carried out at 160°C for 2 hours and then 180°C for 2 hours for the esterification, followed by a polycondensation at 220°C under a pressure of (<500 Pa) for 5 hours, with tetrabutyl titanate (TBT) as a catalyst. Afterward, the oligomer is added to the hard segment oligomer, PBT, and carried out at 240°C for different times [83]. Here, the length of the soft block (PBT30-PBBS) copolyesters, is influenced by polycondensation time. As the polycondensation time increases the transesterification and randomness, crystallization decrease, and results in a balance between tensile strength and elongation, with minimal impact on the thermal stability.

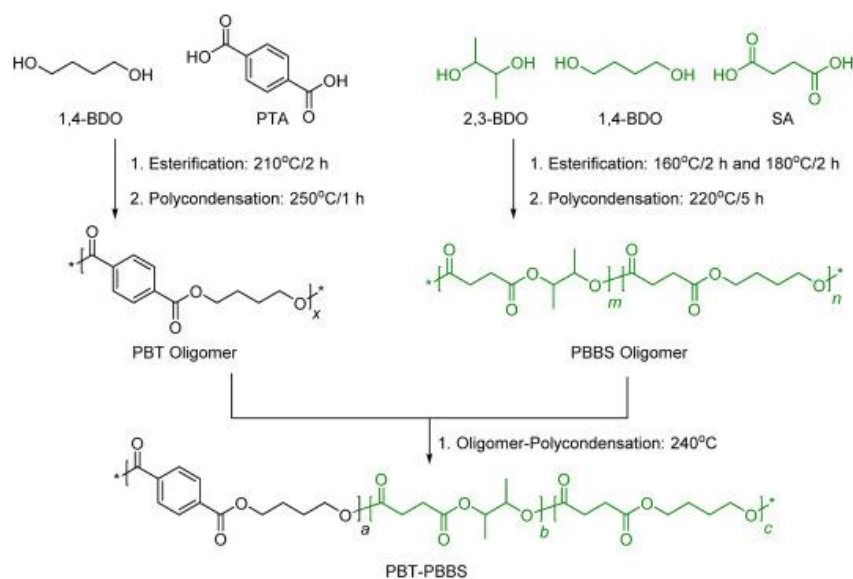


Figure 19: Synthetic route of PBT-PBBS copolyester([83], p. 2)

Overview

The elongation of the soft block significantly influences the final material's properties. Firstly, longer soft blocks reduce compatibility and increase phase separation in polymer mixtures due to the Flory-Huggins interaction parameter. Secondly, the structural properties of the polymer change: increased soft block length results in longer hard blocks, enhancing the polymer's overall properties. This elongation disrupts the crystallization process, leading to a heterogeneous microstructure and decreased glass transition temperature (T_g). Lastly, the mechanical properties are affected. Longer soft blocks reduce crystallinity and phase separation, decreasing tensile strength and modulus but increasing flexibility, impact resistance, and elasticity. Conversely, the elongation of the hard blocks due to elongated soft blocks raises the T_g , melting temperature (T_m), tensile strength, and modulus. By balancing the effects of soft and hard block elongation, polymers can be tailored to meet specific product requirements.

The first objective of this thesis is to synthesize an oligomer from fatty acid dimer diol (FADD) and succinic acid (SA). This is done in a 2:1 and 3:2 FADD:SA ratio to see the influence of the soft block length, but still ensure that a reaction can take place with the rPET afterward. If the soft block is too long, the miscibility, as seen in Figure 14, will cause phase separation, decreasing the final material's properties. On the other hand, the properties might increase if the soft block elongates, this is because of the possible increase of the hard block with it. Both FADD and SA are bio-based products and can be derived from products such as safflowers and corn, making the oligomer a fully bio-based product. The reaction mechanism is given in Figure 20. The oligomers are then tested through $^1\text{H-NMR}$, MALDI-TOF, and GPC to determine their structural properties. By analyzing the results, optimal circumstances for the oligomer synthesis are conducted.

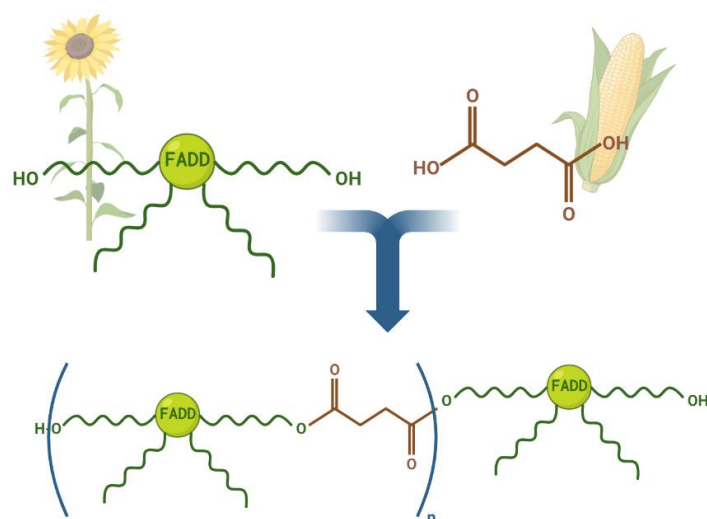


Figure 20: Simplified reaction mechanism for oligomer synthesis from fatty acid dimer diol (FADD) and succinic acid (SA), made with Biorender.com

After the synthesis of the oligomers, it is possible to synthesize a thermoplastic copolyester (TPC). By reacting different amounts of oligomer with waste textile PET (rPET), a range of TPCs is created. As seen from Karanastasis et al., were able to introduce 67wt% of soft block into their polymer [4]. From the theory represented in Figure 14, an elongated soft block makes it possible to use a higher wt% of soft block in the polymer. Therefore, a range of 60-90 wt% is synthesized using both oligomers with a 2:1 and a 3:2 FADD:SA ratio. The reaction mechanism is shown in Figure 21. By incorporating the bio-based oligomer in the PET back bone, the material becomes more sustainable as it eliminates the use of virgin materials by combining a mostly unused waste stream with an oligomer from fully renewable resources into a new valuable TPC material. The structure of the TPCs is analyzed by using various techniques such as ^1H -NMR, ^{13}C -NMR and GPC.

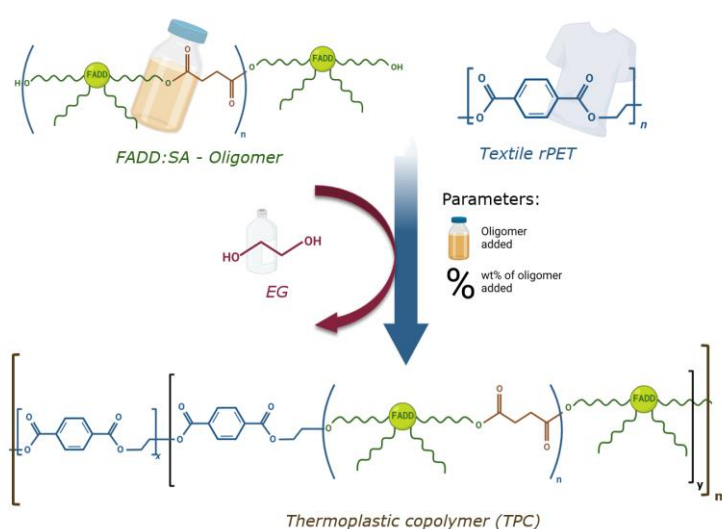


Figure 21: Simplified reaction mechanism for polymer synthesis from the elongated oligomer and waste textile PET (rPET), made with Biorender.com

The synthesized TPCs will then be conducted to thermal and mechanical analysis. To determine the thermal properties (such as melting temperature, crystallization temperature and others) DSC tests are conducted on the different materials. The mechanical properties such as tensile strength and adhesion forces, are analyzed using a tensile tester with different accessories. By doing these tests, it can be determined in which applications the material can be used and how they might be processed.

3 Materials and methods

First, the materials are discussed, followed by the methods of the synthesis and analysis of the oligomer and the polymer are discussed. Then the mechanical testing of the synthesized polymers is followed within this section. For the writing of this master thesis, Grammarly, a free AI writing assistance, was used to check the spelling. To make figures and structures, Biorender.com and Chemdraw Software were used.

3.1 Materials

3.1.1 Reagents and chemicals

For fatty acid dimer diol, the largely available Pripol 1009 by Croda is used. It contains a small amount of isomers, but the main component is shown in Figure 22.

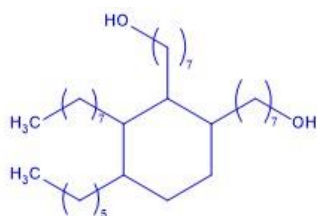


Figure 22: Structural formula of the main isomer in Pripol 1009-LQ-(GD), made with Chemdraw.

The two carboxylic acid functional groups make the Pripol 1009 ideal for an esterification reaction with succinic acid or dimethyl succinate. The succinic acid ($\geq 99.0\%$) used is from ReagentPlus, a trademark from Sigma-Aldrich Co. The dimethyl succinate (98+%) used is from Alfa Aesar, a trademark from ThermoFischer GmbH. It can be synthesized from crops such as corn, making it a bio-based raw material [88]. To improve the possible discoloration of the oligomer, dimethyl succinate can be used as an alternative to succinic acid. The dimethyl succinate (98+%) used is from Alfa Aesar, a trademark from ThermoFischer GmbH. Succinate can be synthesized from SA through a green esterification process [89] or a one-pot synthesis from D-fructose [90].

To accelerate the synthesis of the oligomer, 0.5 wt% of an esterification catalyst can be added to the mixture. The titanium (IV) butoxide (reagent grade 97%) from the company Sigma-Aldrich Co. was chosen to catalyze the reaction. The catalyst is not considered a sustainable product, therefore a reaction without the addition of the catalyst would be a more viable option. But since the catalyst is added in such small amounts, and its influence on the reaction is undeniable, the addition of it is viewed as a parameter.

The hard block in the polymer's backbone is a waste PET (rPET) from textile waste materials provided by Milliken. A small amount of antioxidant (1,3,5-Trimethyl-2,4,6-tris(3,5-di-tert-butyl-4-hydroxybenzyl)benzene (99%) from Sigma) is added to the mixture.

For the catalyst system, two solutions were prepared. The first contains 21 μ l of tetrabutyl orthotitanate (TBT, >97%, Sigma) in 5 ml dry 1-butanol (99%, Acros). The second solution uses 8.68 mg of dried magnesium acetate tetrahydrate (Alfa Aesar) in 5 ml dry methanol (anhydrous, >99%, Sigma).

An excess amount of ethylene glycol (EG, $\geq 99\%$, Sigma) was added to ensure the deconstruction of the rPET material.

3.1.2 Equipment

¹H-NMR spectra were conducted using a JEOL instrument. The GPC data were acquired using an EcoSEC Elite SEC System (Tosoh Bioscience, Germany), with a LenS3 MALS detector (Tosoh Bioscience, Germany) and SecView software V2 (Tosoh Bioscience, Germany). The GPC uses a different chloroform as well (Merck, Germany). MALDI-ToF MS Mass spectra are conducted using a Bruker UltrafleXtreme MALDI-ToF/ToF system.

3.2 Methods

3.2.1 Oligomer synthesis

The following paragraphs discuss the procedures followed, set parameters, and analysis performed in the synthesis of the oligomer.

The oligomers will be coded using the following structure: CODE-(time)h-(temperature). The CODE is defined as the ratio of FADD: SA, F2S1 is a 2:1 FADD:SA ratio, F3S2 is a 3:2 FADD:SA ratio. The addition of the letter *k*, indicates a catalyst was used. The time and temperature can be split, here the first number will refer to the Argon atmosphere and the second to the vacuum atmosphere. For example, F2S1k-(3+2)h-(190+200) means an oligomer with a FADD:SA ratio of 2:1 was made using a catalyst, which reacted 3 hours at 190°C in an Argon atmosphere and 2 hours at 200 °C at Vacuum atmosphere.

Parameters

Different key parameters, including temperature, reaction time, and the addition of a catalyst were varied to determine the optimal conditions. First, the polymerization temperature is set between 180-220°C, this range is above the melting point of the succinic acid (185-187°C), but below the degradation temperature of the oligomer (230-260°C). The reaction time under vacuum and argon are key parameters, with total reaction times ranging from 1 to 7 hours. The ratio of the FADD: SA is varied between a 2:1 ratio and a 3:2 ratio. Another parameter is using either succinic acid or dimethyl succinate to elongate the soft block. Additionally, the impact of adding a catalyst was examined, although it is not a sustainable option. When initial tests successfully produced a longer structure, further tests are conducted with the varied parameters, as shown in Table 1, Table 2, and Table 3.

Table 1: Parameters for the oligomer synthesis using succinic acid without the addition of a catalyst

| Ratio | Time (h) under Argon | Temperature (°C) under Argon |
|--------------|---------------------------------|---|
| 2:1 | 5, 4, 1 | 220 |
| 2:1 | 1, 2 | 200 |
| 2:1 | 7, 6, 4, 3, 1 | 190 |
| 3:2 | 4, 1 | 220 |
| 3:2 | 4, 1 | 190 |

Table 2: Parameters for the oligomer synthesis using succinic acid with the addition of a catalyst

| Ratio | Under Argon | Time (h) Under Vacuum | Total | Temperature (°C) Under Argon | Under Vacuum |
|--------------|------------------------|--------------------------------------|--------------|---|-------------------------|
| 2:1 | 3,2 | 2,3 | 5 | 220 | 190 |
| 3:2 | 3,2 | 2,3 | 5 | 220 | 190 |

Table 3: Parameters for the oligomer synthesis using dimethyl succinate

| Ratio | Catalyst used | Time (h) Under Argon | Under Vacuum | Total | Temperature (°C) Under Argon | Under Vacuum |
|--------------|--------------------------|-------------------------------------|-------------------------|--------------|---|-------------------------|
| 2:1 | no | 1, 4 | / | 1,4 | 180 | / |
| 2:1 | yes | 3 | 2 | 5 | 180 | 220 |
| 3:2 | yes | 3, 2 | 2, 3 | 5 | 180 | 220 |
| 3:2 | yes | 2 | 1 | 3 | 180 | 220 |
| 3:2 | yes | 4, 5 | 3, 2 | 7 | 180 | 220 |

Method

The oligomer was synthesized on a small scale (~3g), using a one-pot condensation polymerization process. The FADD and SA were added to a round-bottom flask, according to the ratio of FADD: SA needed. The experimental setup is shown in Figure 23.

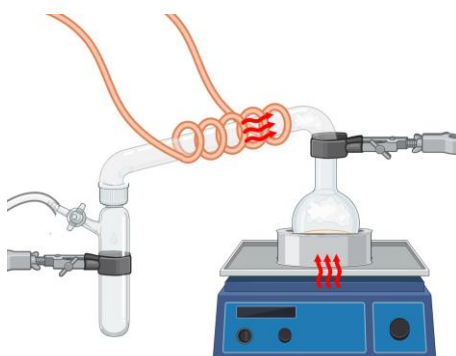


Figure 23: Experimental setup for synthesizing oligomer in a one-pot polycondensation, made with Biorender.com

The mixture was then heated for a certain time under either Argon or Vacuum atmosphere. Afterward, the product was cooled under argon gas to room temperature and stored in a glass container.

Analysis

The oligomers were identified using ^1H nuclear magnetic resonance (^1H -NMR) spectroscopy, gel permeation chromatography (GPC), and matrix-assisted laser desorption/ionization time-of-flight (MALDI-TOF) analysis. ^1H -NMR spectra (JEOL instrument operating at 400 MHz) confirm the formation of the expected oligomer by identifying characteristic peaks, with peak height indicating the amount present. For ^1H -NMR, samples were dissolved in CHCl_3 at concentrations of 10 mg/mL for proton measurements. A good signal-to-noise ratio was achieved with over 64 scans.

GPC provides the molecular mass distribution within the sample, while the MALDI-TOF-tests are used to validate the results obtained from GPC and NMR. The chromatography analysis was performed using an EcoSEC Elite System (Tosoh Bioscience, Germany) equipped with an internal dual-flow differential refractive index (RI) detector and a LenS3 MALS detector (Tosoh Bioscience, Germany). The data were collected and processed using SecView software V2 (Tosoh Bioscience, Germany). Chloroform (Merck, Germany) was used as the solvent and mobile phase at a flow rate of 0.5 mL/min. The pump oven, column oven, and RI detector were all maintained at 40°C. The oligomer samples were dissolved in chloroform at a concentration of ~3,5 mg/mL and filtered through a 0.45 μm PTFE syringe filter before injecting into the column bank. The low-angle detector in the LenS3 MALS detector was used for molecular weight calculations. MALDI-TOF samples are prepared by dissolving 1 drop of oligomer in 2 mL of chloroform (>99%, Sigma) [3].

3.2.2 Polymer synthesis

The following paragraphs discuss the products utilized, procedures followed, set parameters, and analysis performed in the synthesis of the polymer.

The polymers are given a code-name to identify them easily. The code name has the structure of 'POLY-FX XXX -Xwt%'. The middle part of the code name is a reference to the oligomer used, a F2S1k means an oligomer with a FADD:SA ration of 2:1 with a catalyst (k) is used. The last part is the wt% of soft block added. For example, POLY-F3S2k-60wt% is a polymer synthesized using 60 wt% of a 3:2 FADD:SA ratio with catalyst oligomer.

Parameters

The first parameter is the oligomer used in the reaction. The second parameter will be the amount of oligomer (soft block) added to the mixture, to see how the soft block will influence the final polymer that was made. Remembering the research goal, the wt% of the soft block added will be on the higher end, between 60 and 90 wt%.

Method

The polymers were synthesized in a one-pot polymerization condensation on a small scale (~3g). The experimental setup can be viewed in Figure 24.

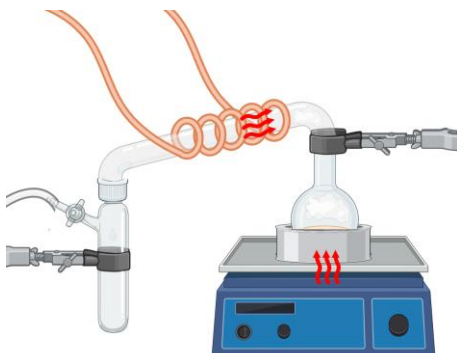


Figure 24: Experimental setup polymer synthesis made with Biorender.com

The mixture will first be heated to 240°C under an Argon atmosphere, where the EG will break down the rPET material into its monomeric parts. When a homogenous mixture is obtained (without the presence of solids), a temperature of 200°C is set and the system is switched from an argon atmosphere to a vacuum distillation for 2 hours. Here the reaction between FADD and EG begins, and EG is removed under vacuum from the mixture into the distillation flask. After the removal of EG, the temperature is increased again to 250°C. In this step the polycondensation of the oligomers into a polymer through transesterification occurs. The polymer gradually becomes more viscous, which complicates the stirring. After a high viscosity is reached that prevents the rotation of the stirrer bar, the mixture is left at 250°C for another hour to ensure more of the oligomers will polycondensate. Afterwards, the material is cooled under an Argon atmosphere to prevent oxidation of the sample. Once cooled down, the polymer is dissolved in chloroform with overnight stirring and precipitated in methanol, as shown in Figure 25. The excess methanol and chloroform are removed and the material is dried overnight in the vacuum oven at 70-75°C to make sure all of the methanol is evaporated from the polymer.

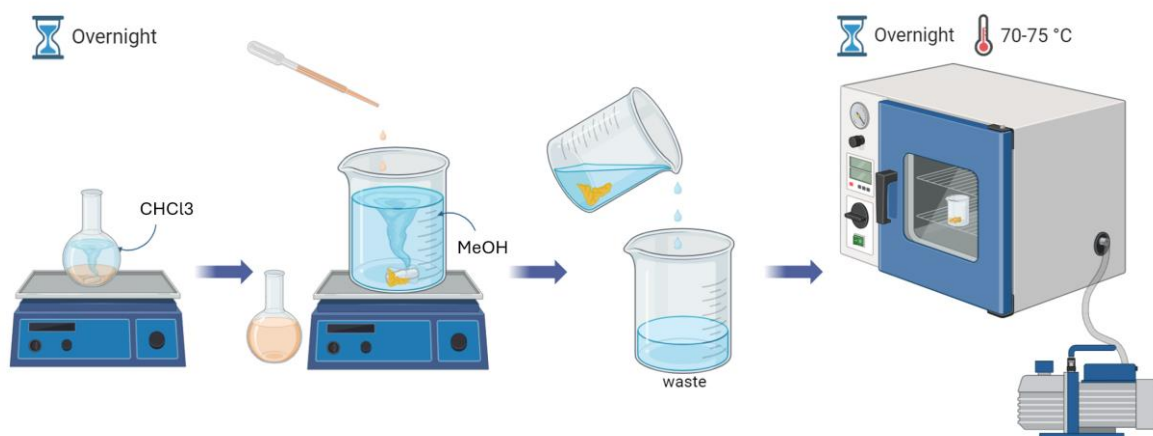


Figure 25: Precipitation and drying process of the polymer overview, made with Biorender.com

Analysis

The results were analyzed using GPC testing to determine the molecular weight distribution in the polymer, these tests are analog as mentioned in 3.2.1 Oligomer synthesis oligomer synthesis. Lastly, ^1H -NMR was conducted, along with ^{13}C Carbon nuclear magnetic resonance (^{13}C -NMR) to get a better understanding of the structures formed in the reaction. The samples were dissolved in CHCl_3 at concentrations of 10 mg/mL for proton and 50 mg/mL for carbon measurements. To facilitate quantitative ^{13}C -NMR, 3-5 mg of relaxation agent $\text{Cr}(\text{acac})_3$ was added before transferring the solutions to the NMR tube.

3.2.3 Characterization of the polymers

The following paragraphs tackle the procedures followed and the set parameters in the mechanical testing of the polymer.

Parameters and preparation of samples

Differential scanning calorimetry (DSC) is used to explore the thermal behavior of the polymer. The measurements occur on a TA Instruments Q20 instrument under N_2 atmosphere using hermetic pans and lids. The DSC was calibrated first, using an indium standard. The samples are prepared by weighing 3-5 mg of polymer into the hermetic pans and pressing them closed. Thermal history was eliminated with an initial isothermal treatment at 280°C for 5 minutes. Both cooling and heating ramps were performed at a rate of $10^\circ\text{C}/\text{min}$. The DSC, equipped with a refrigerated cooling system, had a lower reliable temperature limit of -50°C . The data was collected using the TA Universal Analysis suite, which provided values for T_g , T_m , T_c and ΔH_m [3].

First, the polymers are put into a heating hydraulic pressing machine (PCH- 600DG heat hydraulic press from Tianjin Pinchuang Technology Development Co.). The polymer is taken out of the square mold and tensile specimens are pressed using a Ray-ran cutting press with a dog bone-shaped cutter, the average specimen dimensions are given in Figure 26.

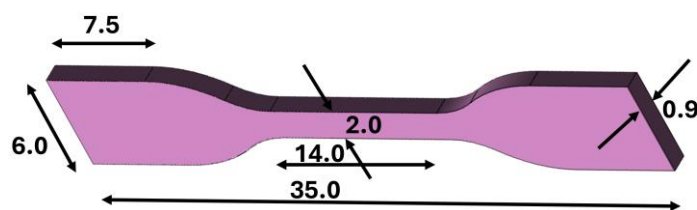


Figure 26: Dimensions of tensile specimen in mm [modified from [91]]

For the peel adhesion tests, 1MM strips were cut and weighed from ASTERA polyester foils, clear transparent PET film $125\ \mu\text{m}$, untreated. The polymers are dissolved in a small amount of chloroform and spread on the strips by using the K Hand coater with a K bar of wire diameter 1.27 mm. The strips are then covered with aluminum foil to prevent dusting and air dried for 2 days.

Methods

Next, tensile tests were conducted on the Shimadzu AGS-X series precision universal tester, using pneumatic grips and fitted with tensile clips and a 5 kN load cell. It is important to note that the materials may not show any air bubbles or other imperfections, as they can influence the tensile tests. The samples are placed between the pneumatic grips where the tensile testing will occur. The distance traveled by the grips was measured as the extension. Samples that showed a break outside the central gauge, or at an imperfection, were excluded from the measurement. For each sample 6 test specimens were conducted to assess the standard deviation in the reported values.

For the peel adhesion testing, the same universal tester is used, combined with a 90 degree peel tensile jig (THS1605-1kN-50x30-BD) and a 500 N load cell. The prepared strips are placed on the aluminum carrier plate and rolled to ensure sticking. Next, part of the strip without any polymer is pulled between rods and placed between the pneumatic grip of the tensile tester. The strip is pulled at a constant speed of 305 mm/min. The peel adhesion test setup is given in Figure 27.

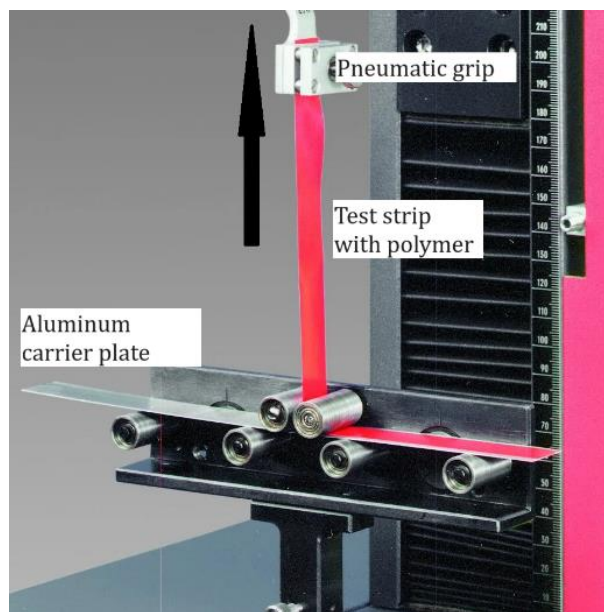


Figure 27: Peel adhesion test set up with different parts marked (modified from [92])

4 Results and discussion

In this section, the results will be discussed. First, the analysis results, including the ^1H -NMR, GPC and MALDI TOF experiments, of the oligomer synthesis is reviewed and followed by the analysis results, including the ^1H -NMR, C-NMR, and GPC, of the polymer synthesis. Lastly, the results of the physical and mechanical properties of the polymers are given, including the DSC and tensile test results.

4.1 Oligomer synthesis

First, the ratio of FADD:SA in the oligomers is varied between 2:1 and 3:2, referred to as F2S1 and F3S2. A second parameter is the addition of a TBT catalyst to the oligomer, referred to with the letter k. Lastly, the effect of the reaction temperature and time is discussed by varying them between 190°C - 220°C and 1 to 7 hours. To analyze the oligomers ^1H -NMR, GPC and MALDI-TOF tests are conducted. From the ^1H -NMR the actual ratio between FADD:SA can be estimated, as well as a notion about the structure of the oligomer. GPC tests build further on the calculated ratio from the ^1H -NMR tests by investigating the different lengths of oligomers being formed. Additionally, MALDI-TOF experiments were conducted to show the higher ratios of FADD:SA formed in the reaction. The synthesis reaction is shown in Figure 28.

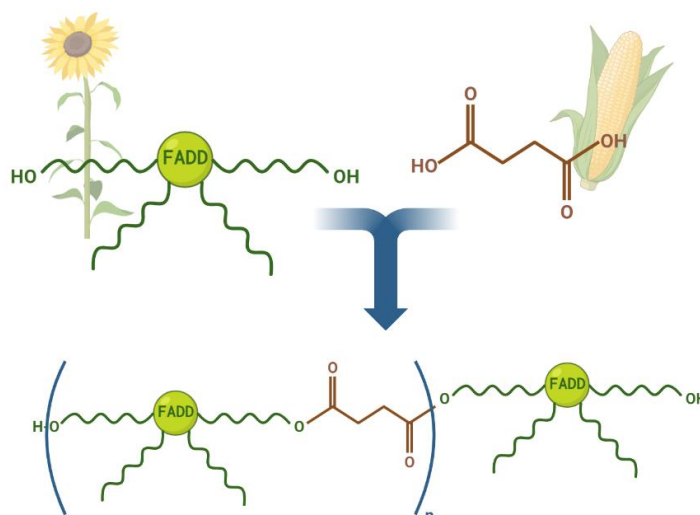


Figure 28: Representation of reaction for the synthesis of the oligomer with FADD and SA, made with Biorender.com

4.1.1 ^1H -NMR

^1H -NMR is conducted to investigate the chemical structure of the oligomer, as well as calculating the average ratio formed within the structure. In Figure 29 an analysis of the ^1H -NMR spectrum is made.

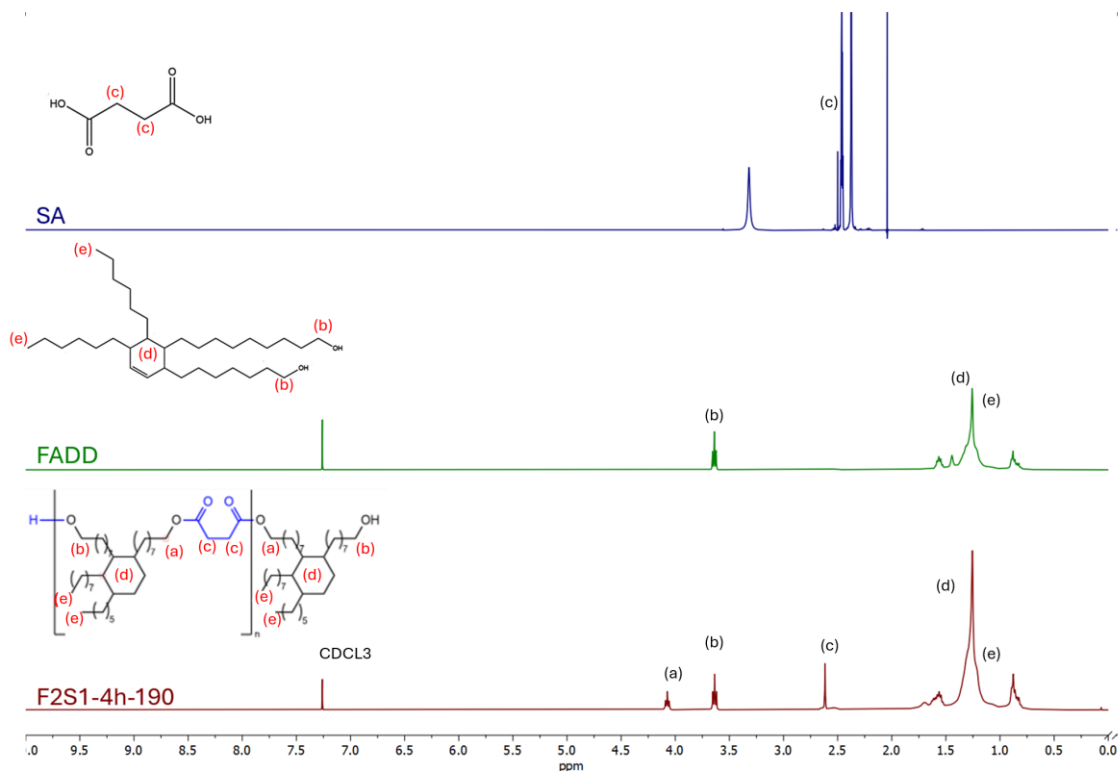


Figure 29: ^1H NMR spectra of pure SA, pure FADD, and, a 2:1 ratio oligomer with corresponding structures

A blank sample of pure FADD and pure SA is measured to analyze the spectra of the oligomers, which can be seen in Figure 29. The peak of 2.62 ppm corresponds to the protons present in succinic acid. The peak at 4.07 ppm is equivalent to the methylene protons next to the ester bond between FADD and SA. The peaks in the area between 1.75 and 0.75 ppm correspond to the aliphatic protons of pure FADD, as its equivalent to the one the spectrum of pure FADD. The spectrum of oligomer F2S1-4h-190 shows that the FADD and SA reacted, as peak (a) at 4.08 ppm appears on the spectrum. This peak corresponds to the protons on the newly formed bond between the FADD molecule and SA molecule. The surface covered underneath the peaks of a ^1H NMR spectra coincides with the amount of that type of proton present.

In Figure 30 the impact of reaction temperature and time on the final oligomer is investigated.

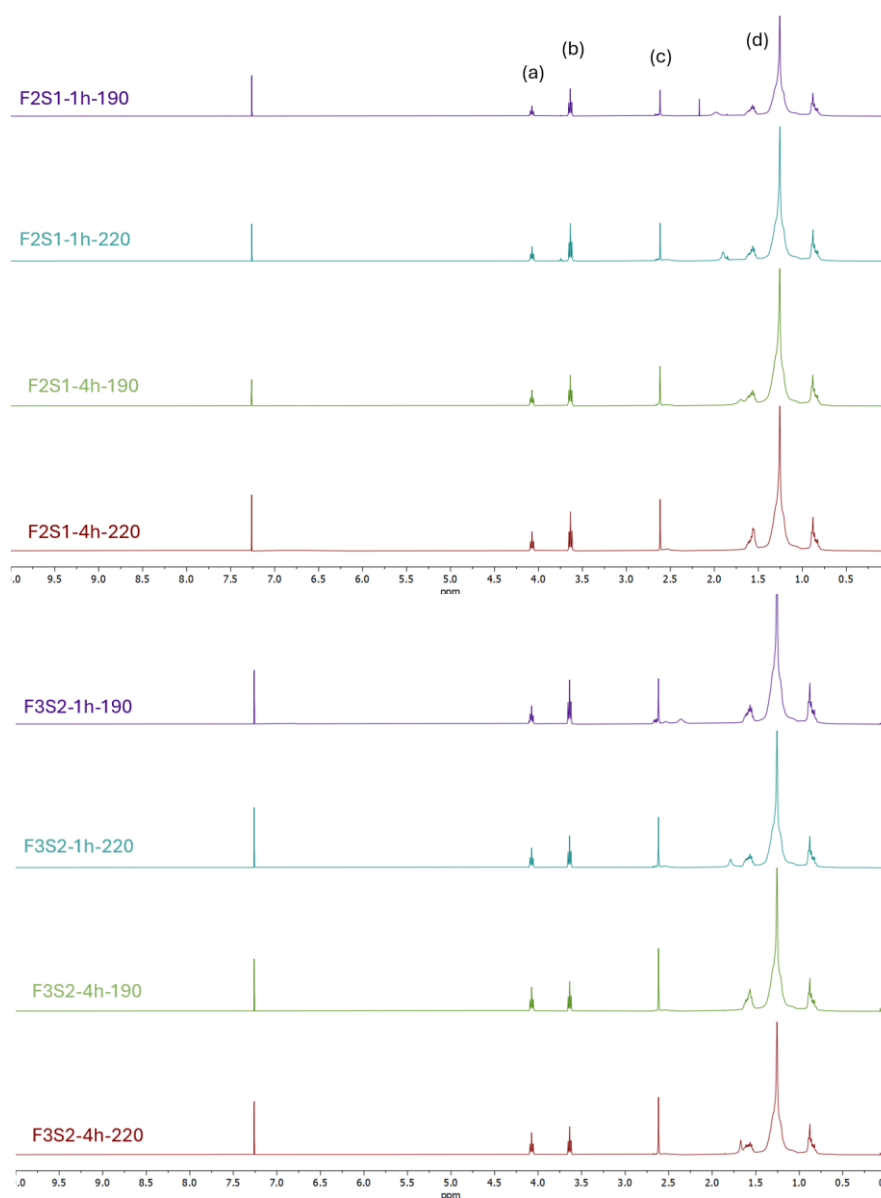


Figure 30: ¹H-NMR spectra of oligomers with different temperatures (190 and 220°C) and reaction times (1h and 4h) of the 2:1 FADD:SA ratio, and 3:2 FADD:SA ratio oligomers

The integrals are measured in ratio to the integral of peak (a) being 1.00, and given in Table 4.

Table 4: Integrals of peaks from ^1H -NMR spectra of oligomers with different temperatures and reaction times

| Oligomer | Peak (a) | Peak (b) | Peak (c) | Peak (d) |
|-------------|----------|----------|----------|----------|
| F2S1-1h-190 | 1.00 | 2.14 | 2.11 | 56.02 |
| F2S1-1h-220 | 1.00 | 2.20 | 1.95 | 54.83 |
| F2S1-4h-190 | 1.00 | 1.65 | 1.74 | 50.67 |
| F2S1-4h-220 | 1.00 | 1.68 | 1.69 | 49.30 |
| F3S2-1h-190 | 1.00 | 1.78 | 1.41 | 46.38 |
| F3S2-1h-220 | 1.00 | 1.34 | 1.62 | 40.42 |
| F3S2-4h-190 | 1.00 | 1.10 | 1.50 | 37.07 |
| F3S2-4h-220 | 1.00 | 1.06 | 1.51 | 37.66 |

The ratio of the oligomers can be determined from the ^1H -NMR spectra as follows. The structure of the oligomer (Figure 31) indicates that the number of hydroxylic groups relative to the number of bonds formed between the succinic acid and the fatty acid is proportional to the oligomer ratio. The integral of the peak around 3.63 ppm is a measure of methylene protons next to the hydroxyl group. The integral of the peak around 4.08 ppm is an indicator of the number of bonds formed between the FADD and SA sections of the oligomer. Figure 31 gives a schematic representation of the 3:2 FADD:SA ratio.

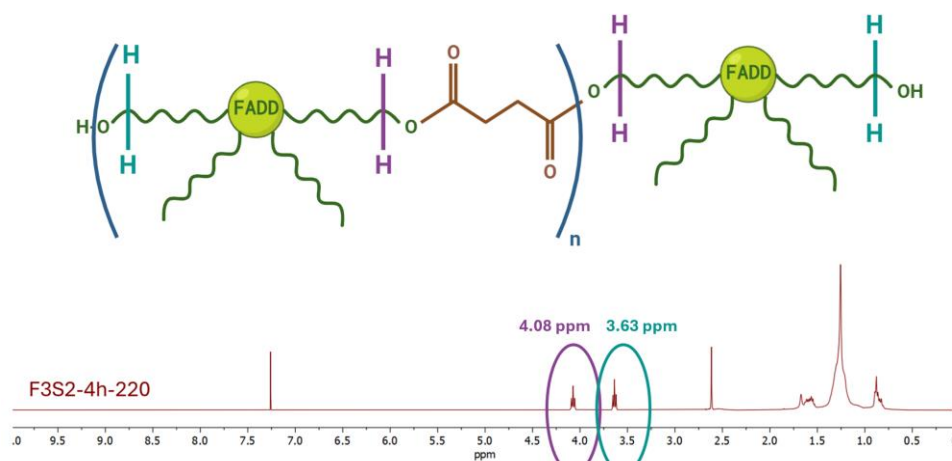


Figure 31: Schematic representation of the oligomer structure with protons for further calculations marked.

As shown in Figure 31, 4 methylene protons next to the hydroxyl group of the FADD as well as 4 on the bonds between FADD and SA. The ratio can be calculated with the following formula.

$$\text{ratio value} = \frac{\int \text{peak } 4.08 \text{ ppm}}{\int \text{peak } 3.64 \text{ ppm}}$$

As an example, the calculation of the ^1H -NMR spectrum of F3S2-4h-220 is made.

$$\text{ratio value}_{\text{calculated}} = \frac{\int \text{peak } 4.08 \text{ ppm}}{\int \text{peak } 3.64 \text{ ppm}} = \frac{1.00}{1.06} = 0.943$$

The expected ratio value for a 2:1 ratio would be 1.00, as the structure includes four protons on the bonded carbons and four methylene protons adjacent to the hydroxyl groups. For a 3:2 ratio it would be 2.00. When the calculated ratio value is lower than the expected value, it indicates that the reaction mixture is incomplete and a substantial amount of unreacted FADD remains in the oligomer. When it is larger, a large number of longer oligomers are formed. The ratios calculated are an estimation of the average value, there will be oligomers that are longer and shorter in the mixture. Table 5 presents the ratio values calculated for the spectra shown in Figure 30. The ratio values for other oligomers, varying between 1 hour and 7 hours reaction time, are provided in Table 5 for reference.

Table 5: Ratio values calculated from ^1H NMR spectra of the oligomers shown in Figure 30.

| Oligomer | Ratio value | Oligomer | Ratio value |
|--------------------|--------------------|--------------------|--------------------|
| <i>F2S1-1h-190</i> | 0.467 | <i>F3S2-1h-190</i> | 0.562 |
| <i>F2S1-1h-220</i> | 0.455 | <i>F3S2-1h-220</i> | 0.746 |
| <i>F2S1-4h-190</i> | 0.606 | <i>F3S2-4h-190</i> | 0.909 |
| <i>F2S1-4h-220</i> | 0.595 | <i>F3S2-4h-220</i> | 0.943 |

The ratio values of the oligomer synthesized, without a catalyst, indicate that a significant amount of unreacted FADD remains in both the 2:1 and 3:2 FADD:SA ratios. The values increase significantly with longer reaction times. The temperature, however, appears to have less impact, as the differences are smaller with extended reaction times. With shorter reaction times, temperature has a greater effect on the ratio value. Additionally, the 3:2 FADD:SA ratio oligomer shows more variation with changing parameters than the 2:1 ratio variant. Overall, it can be concluded that the longer reaction times, and to a lesser extent higher temperatures, result in more FADD reacting with succinic acid. Furthermore, the 2:1 FADD:SA ratio appears to be more consistent than the 3:2 FAD:SA ratio oligomers, as their ratio value is more stable under different reaction circumstances.

When a catalyst is added to the oligomer synthesis and the reaction is conducted partly under an argon atmosphere and partly under a vacuum, the ratios are improved significantly as shown in the spectra in Appendix 2. The calculated values are given in Table 6.

Table 6: Ratio values calculated from the ^1H -NMR spectra of the oligomers with the addition of a catalyst

| Oligomer | Ratio Value | Oligomer | Ratio Value |
|-------------------------------|--------------------|-------------------------------|--------------------|
| <i>F2S1-5h-220</i> | 0.735 | <i>F3S2-4h-220</i> | 0.909 |
| <i>F2S1k-(3+2)h-(190+220)</i> | 1.28 | <i>F3S2k-(3+2)h-(190+220)</i> | 2.04 |
| | | <i>F3S2k-(5+2)h-(190+220)</i> | 1.67 |

When the oligomers are synthesized with a catalyst, the ratio values reach their expected results of 1.00 for a 2:1 ratio and 2.00 for a 3:2 ratio. This indicates a nearly complete reaction of FADD when a catalyst is added, in a synthesis with a total reaction time of 5 hours (2 hours under argon and 3 hours under vacuum). Extending the reaction time beyond 5 hours does not yield significant improvements, suggesting that 5 hours is optimal. Based on the obtained results, oligomers are synthesized for polymerization with PET using a catalyst, first reacting at 190°C under Argon atmosphere for 2 hours, followed by a reaction at 220°C under Vacuum atmosphere for 3 hours.

For polymer synthesis, a higher volume of oligomers (10 grams) was required. The ratio values are given in Table 7, the ^1H -NMR spectra are shown in Appendix 3.

Table 7: Ratio values calculated from the ^1H -NMR spectra of the oligomers used for polymer synthesis

| Oligomer | Ratio Value |
|------------------------------|--------------------|
| <i>F2S1k-(2+3)-(190+220)</i> | 1.11 |
| <i>F3S2k-(2+3)-(190+220)</i> | 2.17 |

Both oligomers have ratio values relatively close to their suspected ratio and can be used for polymer synthesis.

1.1.2 GPC

GPC tests were conducted on the oligomers to investigate the different lengths formed in the synthesis. The GPC results of the oligomers synthesized to determine the influence of the reaction temperature and time, are given in Figure 32.

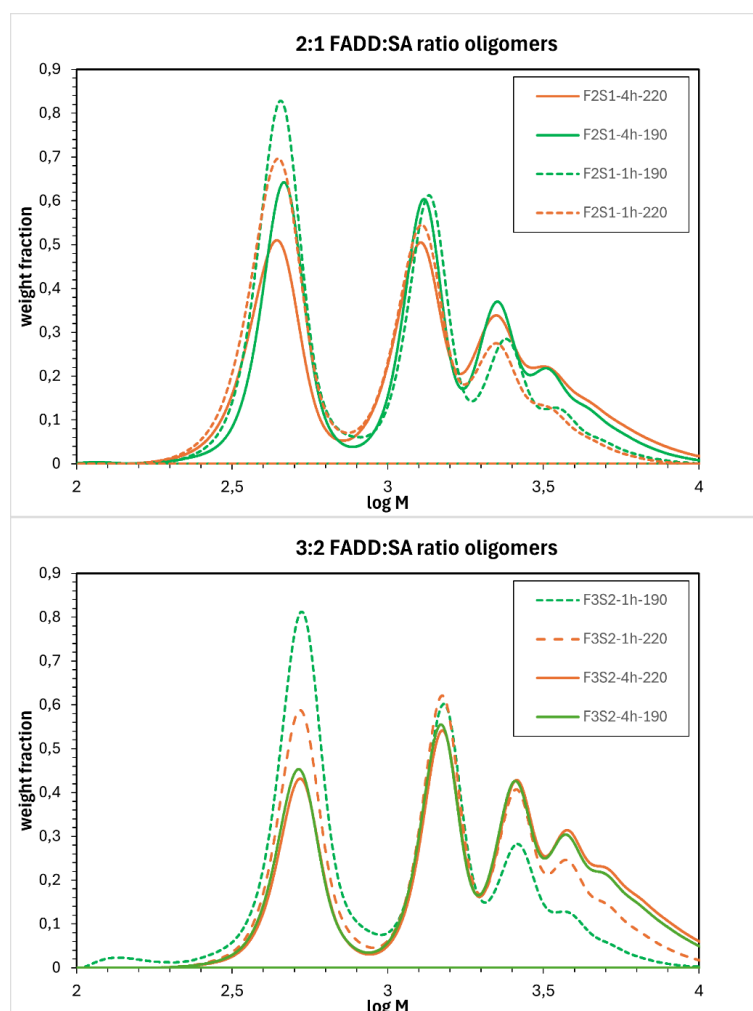


Figure 32: Molecular weight distributions of selected samples from GPC measurements. (upper) 2:1 FADD:SA ratio oligomers (lower) 3:2 FADD:SA ratio oligomers

A 2:1 FADD:SA ratio oligomer has an expected molecular weight of 1218 g/mol or $\log M = 3.09$ (FADD ~ 550 g/mol, SA ~ 118 g/mol), a 3:2 FADD:SA ratio oligomer has one of 1886 g/mol or $\log M = 3.28$. From the GPC data in Figure 32 a first peak is visible around a value of $\log M$ is 2.7, which corresponds to a molecular weight of 500 g/mol from the unreacted FADD. The second peak at $\log M = 3.10$, aligns with the expected value for a 2:1 FADD:SA ratio oligomer. A third peak at a $\log M$ of 3.35 or molecular weight of 2240 g/mol for a 3:2 FADD:SA ratio. There are peaks corresponding to an even higher molecular weight apparent. The same peaks are visible for the 3:2 FADD:SA ratio oligomers but differ in height among the same ratio. It is clearly noticeable that the first peak decreases with an increasing reaction time while the last peaks increase. A higher number of FADD molecules react with SA and form larger oligomers. The temperature makes a bigger difference between oligomers with a reaction time of 1 hour instead of 4 hours. However, a higher reaction temperature is better as the molecules get more energy to interact. The temperature difference even increases in the 3:2 FADD:SA ratio, when compared to 2:1 FADD:SA ratio.

The addition of a catalyst to the mixture increases the amount of FADD reacting with SA. As the peak at $\log M = 2.07$ decreases, and peaks at higher values increase, more FADD reacts with SA forming oligomers. When Figure 33 gives an indication of the estimated molecular weight synthesized.

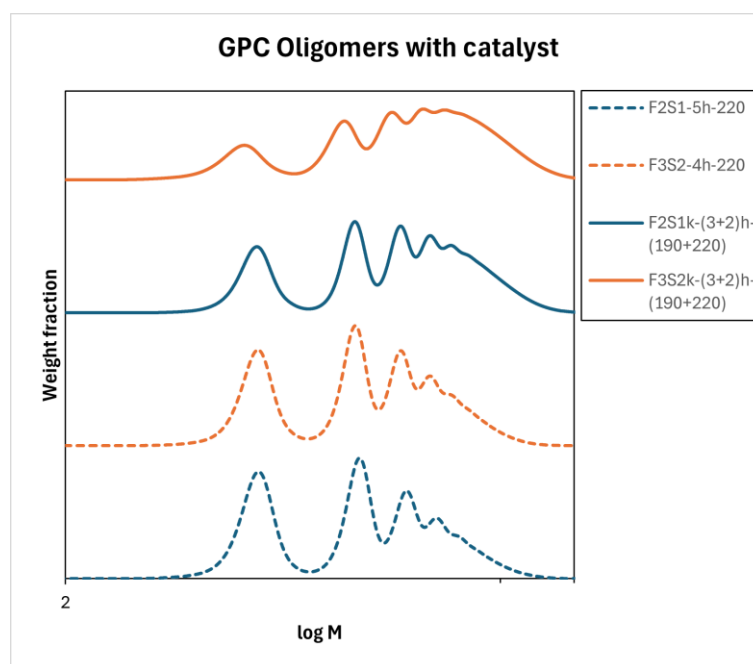


Figure 33: Molecular weight distributions of selected samples from GPC measurements, differing between oligomers synthesized without a catalyst (dotted line), and an equivalent oligomer with the addition of a catalyst (full line)

The amount of FADD that reacts is significantly higher when a catalyst is added. The addition does not only increase the amount of 2:1 and 3:2 ratio, but higher ratios such as 4:3 and 5:4 increase as well. The conclusions from GPC data are consistent with the results from $^1\text{H-NMR}$ data.

4.1.3 MALDI-TOF

The GPC measurements showed that adding a catalyst increased the amount of higher FADD:SA ratios formed in the oligomers. MALDI-TOF measurements were conducted to see which ratios are formed in the oligomers. The spectrum of sample F2S1k-(3+2)h-(190+220) is given in Figure 34.

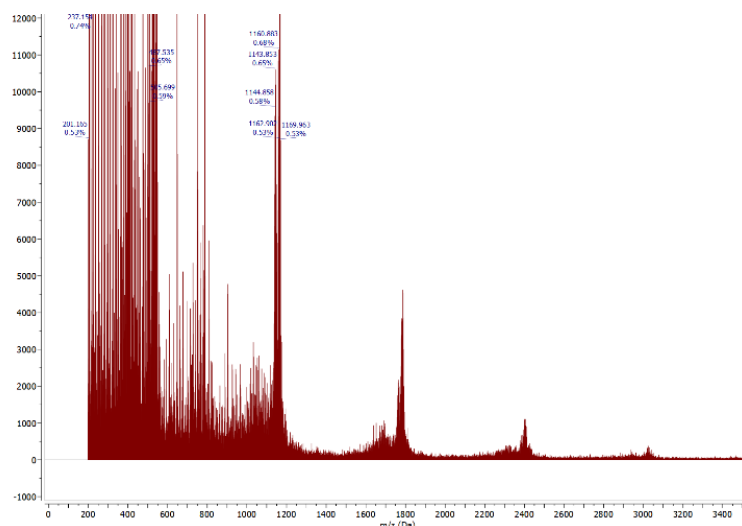


Figure 34: Molecular weight distributions measured with MALDI-TOF of sample F2S1k-(3+2)h-(190-220)

The MALDI spectra confirms what was seen in the GPC measurements. A large number of peaks is visible at 550 Da (~ 550 g/mol) to 1220 Da (~ 1220 g/mol), corresponding to the unreacted FADD and 2:1 ratio being present. A group of peaks around 1800 g/mol aligns with the 3:2 ratio oligomer. Peaks at 2400 g/mol and 3000 g/mol, matching the 4:3 and 5:4 ratio are represented in the MALDI-TOF spectra as well.

4.2 Polymer synthesis

To investigate the polymers when the soft block is increased, two series of polymers are synthesized. The first series is made using a 2:1 FADD:SA oligomer with added catalyst. The second series, uses a 3:2 FADD:SA oligomer with added catalyst. Both oligomers reacted 2 hours in a argon atmosphere at 190 °C, and were then switched to a vacuum atmosphere in which they stayed 3 hours at 220°C before ending the reaction. The polymer series both contain a range of polymers in which the wt% soft block differs from 60 up to 90%. The polymers were synthesized as described in 3.2.2 Polymer synthesis. The polymers were then analyzed using ^1H -NMR and ^{13}C -NMR to give notion of the structures being formed, as well as calculate an estimation of the actual wt% of soft block in the polymer. GPC measurements on the polymer, give the molecular weight distribution of the polymer. The reaction mechanism is shown in Figure 35.

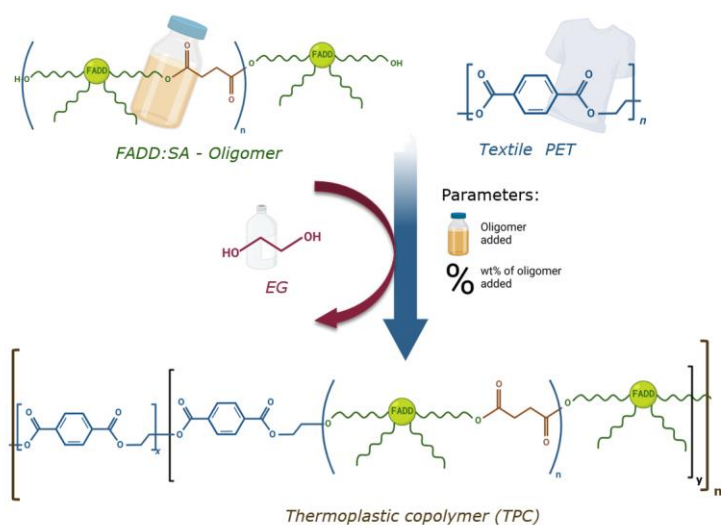


Figure 35: Synthesis of TPC from FADD:SA-oligomer and Textile rPET, made with Biorender.com

4.2.1 ^1H -NMR

Analogue to the oligomers, the structure of the polymers can be determined with ^1H -NMR. The structure of the TPC can be analyzed using the peaks, which is represented in Figure 36.

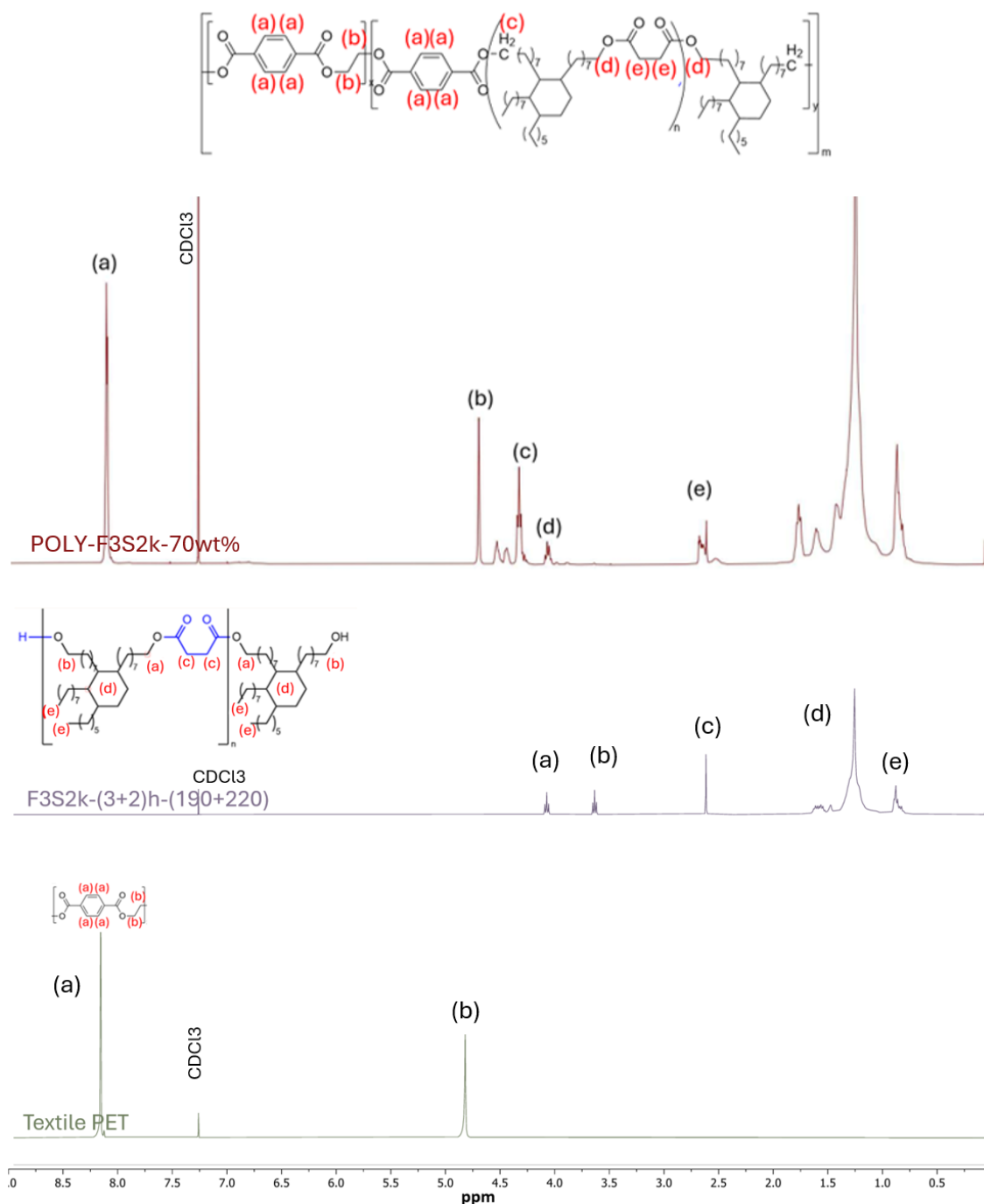


Figure 36: ^1H -NMR spectra of (top) a formed TPC with corresponding structure and marked peaks, (middle) the used oligomer, and (bottom) the waste textile PET material

As seen in the ^1H -NMR from the soft block, the larger 3 peaks around 1.20 ppm come from the FADD present in the soft block of the TPC. Peak (a) at 8.09 ppm corresponds to protons on the terephthalate ring present in the hard segment. The next peak (b) at 4.69 ppm correlates with the protons of the oxyethylene units of PET where an ethylene glycol (E) stands between two terephthalic acids (T), forming a TET segment. Its associated peaks (b') at 4.53 ppm and (b'') at

4.43 ppm, prove transesterification takes place, as ethylene glycol (E) can be in between a terephthalic acid (T) and succinic acid (S) or between two succinic acids, forming SET, TES segments and SES segments. Peak (c) at 4.33 ppm correlates with the methylene protons of the bond between fatty acid dimer diol (F) and terephthalic acid (T). Peak (d) at 4.07 ppm is compatible with the protons on the fatty acid dimer diol (F) next to succinic acid (S). The last peak (e) at 2.67 ppm is for the methylene protons on the ester bond between succinic acid (S) next to a fatty acid dimer diol (F). Its associated peak (e') again proves transesterification when succinic acid (S) lies next to ethylene glycol (E), forming ESE, ESF, FSE sequences. Transesterification is a chemical reaction where ester bonds are exchanged between molecules, rearranging the polymer chains. This can disrupt the regular structure needed for crystallization, as it can prevent the formation of well-defined hard blocks and therefore, other structures are formed as well.

First, the difference between the used oligomers to create the polymers is investigated. The spectra are represented in Figure 37. The values of the integrals of the peaks marked are given in Table 8.

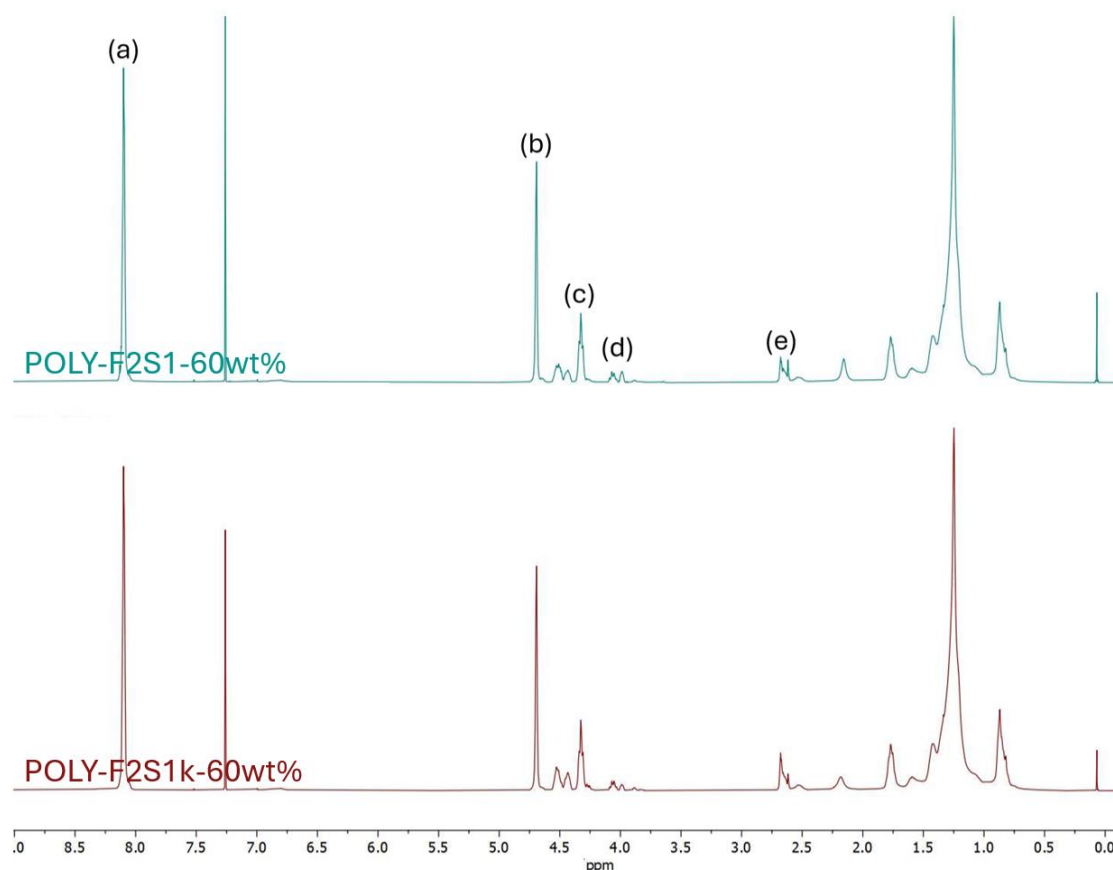


Figure 37: Representative ¹H-NMR spectra of polymers synthesized from (top) F2S1 oligomer without catalyst and, (bottom) F2S1 oligomer with addition of catalyst

Table 8: ^1H -NMR integral values of the peaks marked in Figure 37, from polymers with 60wt% of soft block added

| Peak | ppm | Integral of peak |
|--|------|------------------|
| TPC from oligomer F2S1-7h-190 with 60wt%SB | | |
| a | 8.09 | 1.00 |
| b | 4.69 | 0.54 |
| c | 4.33 | 0.31 |
| e | 2.67 | 0.17 |
| TPC from oligomer F2S1k-(3+2)h-(190+220) with 60wt%SB | | |
| a | 8.09 | 1.00 |
| b | 4.69 | 0.52 |
| c | 4.33 | 0.31 |
| e | 2.67 | 0.22 |

From this ^1H -NMR no significant difference is noticeable between the synthesized polymers. This is unexpected as is seen in 4.1.1 ^1H -NMR, without a catalyst there is still a large amount of unreacted FADD represented. This can suggest that unreacted FADD from the oligomer has reacted with PET and formed other sequences such as TFT. To get a better grip on the molecular structure, ^{13}C -NMR tests were conducted as well. The ^1H -NMR spectra of the TPCs made from different oligomers are given in Appendix 4. To situate the influence of the soft block wt% on the polymers microstructure, ^1H -NMR tests were conducted on two sets of polymers. The first set used a 2:1 FADD:SA ratio oligomer; the second set a 3:2 FADD:SA oligomer. Both sets cover different SB wt% from 60 up to 90 wt%. The spectra is shown in Figure 38, and Figure 39.

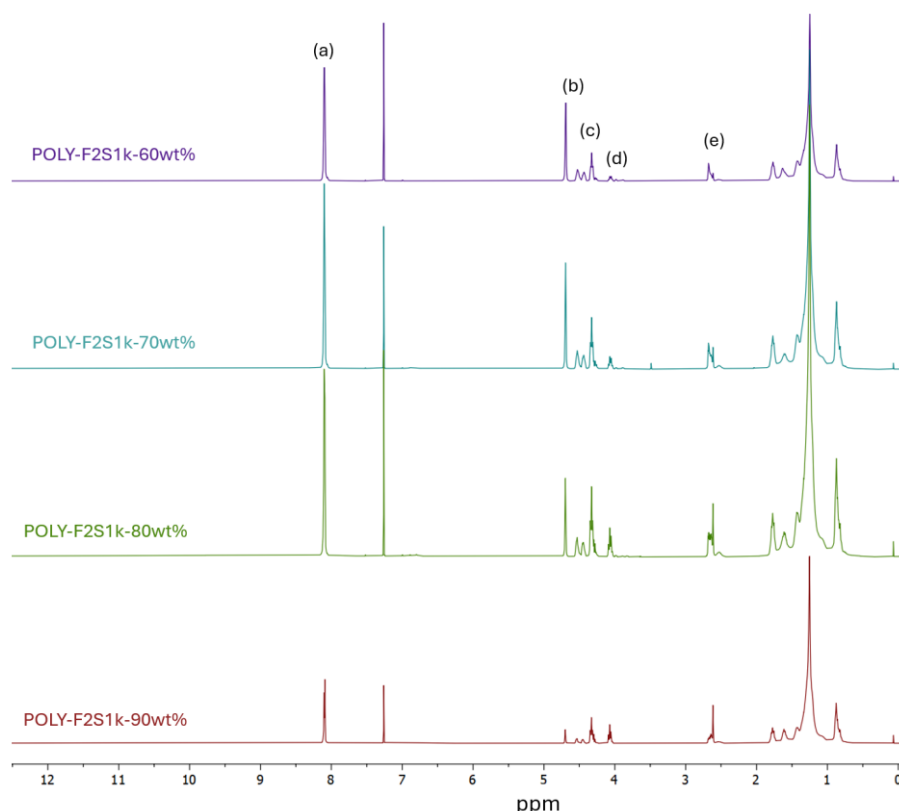


Figure 38: Representative ^1H -NMR spectra of polymers synthesized from rPET with 2:1 FADD:SA ratio oligomers

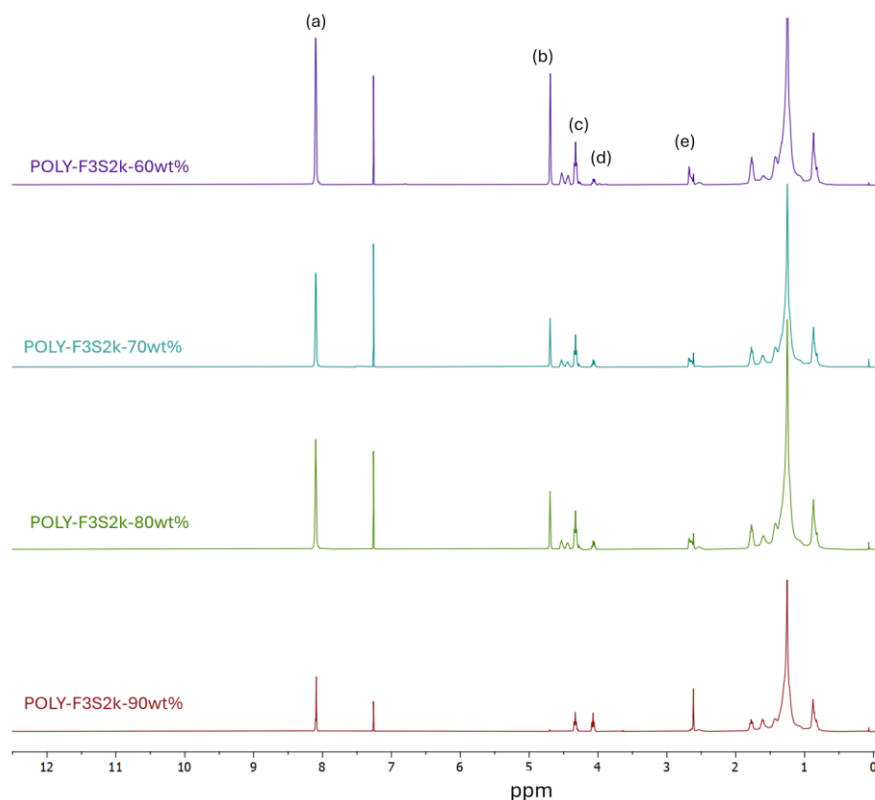


Figure 39: Representative ^1H -NMR spectra of polymers synthesized from rPET with 3:2 FADD:SA ratio oligomers

By comparing the peaks from the different spectra shown Figure 39 and Figure 39, it can be seen that polymers with a higher SB wt% are synthesized. For example, with higher SB wt% the height of peak (b) decreases, meaning that the amount of TET segments decreases and therefore the length of the hard block decreases as well. Peak (e) increases when the SB wt% increases, meaning more bond between succinic acid and fatty acid dimer diol are formed. From peak (a) can be concluded that a hard block is formed. This is visible in the polymer range made with a 2:1 FADD:SA oligomer, as well as the polymer range made with a 3:2 FADD:SA oligomer. However, it seems more significant in the 2:1 FADD:SA range than the 3:2 FADD:SA range. This can be due to poor miscibility causing phase separation, leading to less effective bonds between succinic acid and fatty acid dimer diol and, between oligomer and hard block. This supports the theory from in Figure 14.

4.2.2. ^{13}C -NMR

^{13}C -NMR tests were conducted to do a microstructure analysis of the polymers. Since transesterification can occur, as seen from ^1H -NMR results, different sequences can be formed as shown in Figure 40.

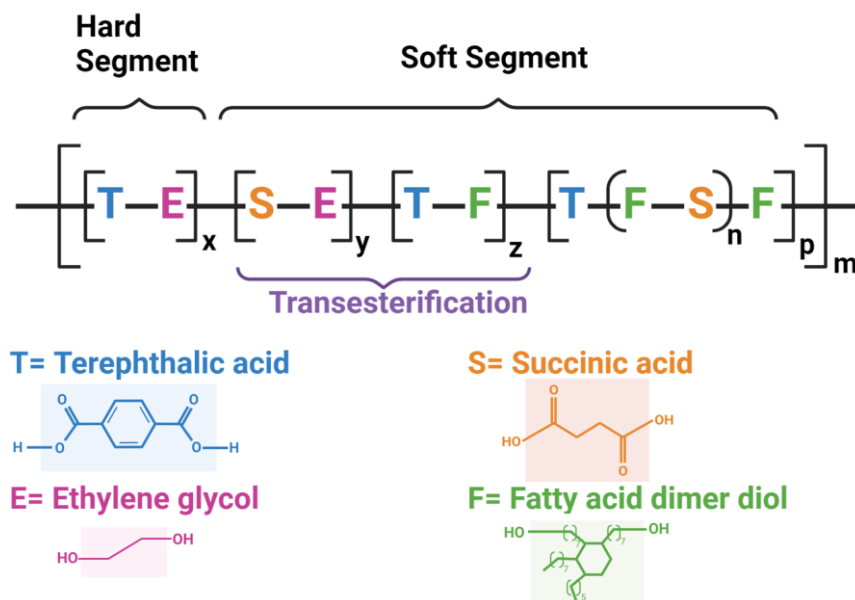


Figure 40: Soft block of the TPC with all possible sequences shown in one figure all together.

The key areas of the ^{13}C -NMR tests are marked in Figure 41, and enlarged in Figure 42.

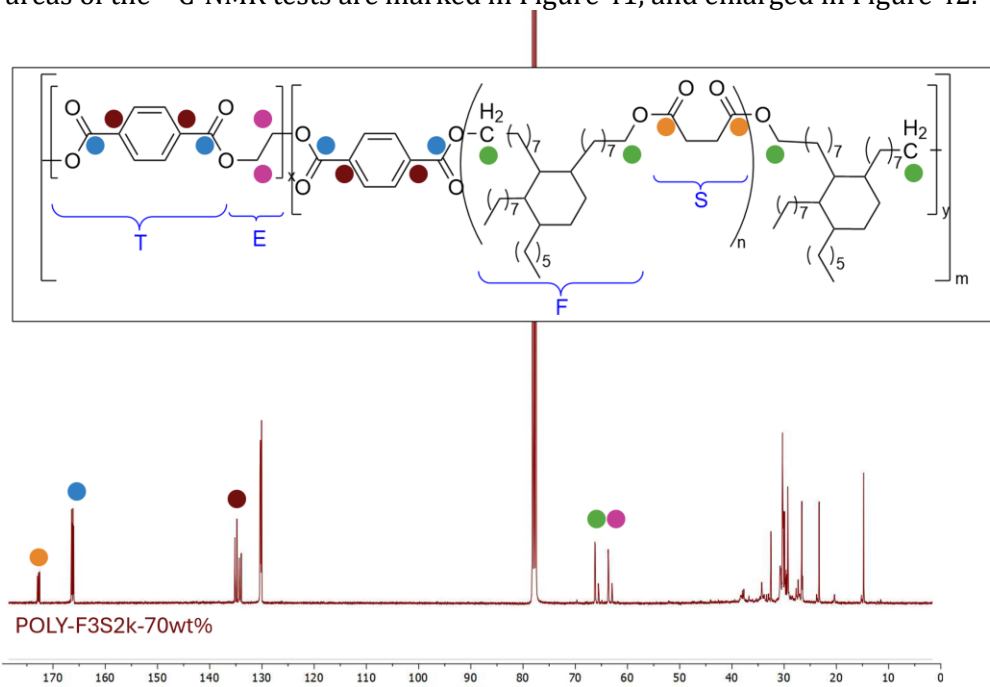


Figure 41: Selected ^{13}C -NMR spectra, with the key regions from the different segment distributions marked as shown in accompanying polymer structure, with T= terephthalic acid, E= ethylene glycol, F= fatty acid dimer diol, and S= succinic acid.

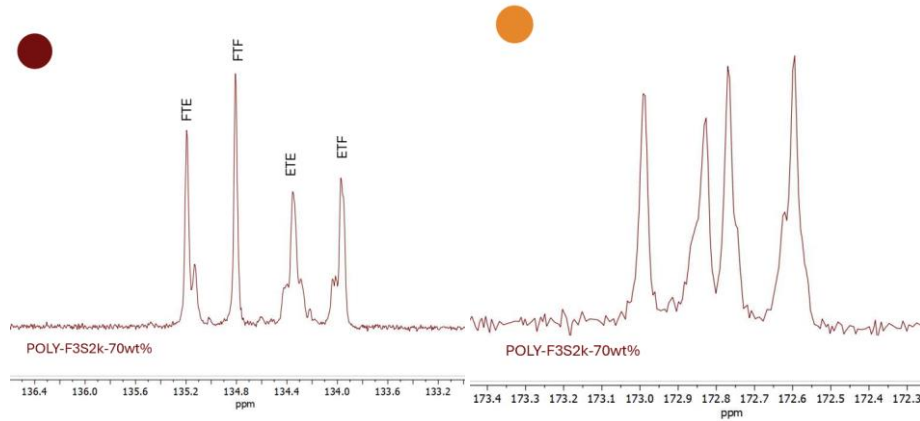


Figure 42: Summary of ^{13}C -NMR spectra of TPCs with magnifications of the key areas for sequence analysis. (left) represents the sequences FTE, FTF, ETE, and ETF, which can be used for hard block length calculations. (right) represents the sequences FSE, FSF, ESE, and ESF, which proves the presence of transesterification.

From the ^{13}C -NMR spectra, the average length of the hard block can be estimated. First, the mole fraction of the TET dyads and TEF/FET dyads are calculated, and its sequence analysis magnification is given in Figure 42.

$$N_{ETE} = \frac{\int ETE}{\int FTE + \int FTF + \int ETE + \int ETF} = \frac{1.28}{1.00 + 0.989 + 1.28 + 1.08} = 0.294$$

$$N_{ETF/FTE} = \frac{\int ETF + \int FTE}{\int FTE + \int FTF + \int ETE + \int ETF} = \frac{1.08 + 1.00}{1.00 + 0.989 + 1.28 + 1.08} = 0.478$$

The average length of the hard block can be calculated from these mole fractions.

$$L_{HB} = \frac{N_{ETE} + 0,5 * N_{ETF/FTE}}{0,5 * N_{ETF/FTE}} = \frac{0.294 + 0.239}{0.239} = 2.23$$

This is corresponding to the research of Karanastasis A. et al., a TPC consisting of 60 wt% SB, the hard block has an average length of 3.4 [4]. TPCs from 50wt% SB and 37wt% SB showed an average length of 4.6 and 7.8 respectively. As the soft block content for this sample is increased to 70wt%, the result of 2.23 falls within the line of what Karanastasis et al. reported. The idea of creating a longer hard block as the soft lock length increases is contradicting with these results. However, this can be explained by the transesterification that occurs, complicating the situation.

The ^{13}C -NMR spectra can prove there is transesterification present in the polymer. The fact that four peaks are present at the specific range between 172.5 ppm to 173.1 ppm, shows that the sequences (FSE, FSF, ESE, ESF) are all present. The magnification of the FSF dyads are given in Figure 42.

4.2.3 GPC

To analyze the molecular weight distribution within the polymer, GPC tests were conducted on the polymer materials. The results are graphically given in Figure 43, and displayed in Table 9.

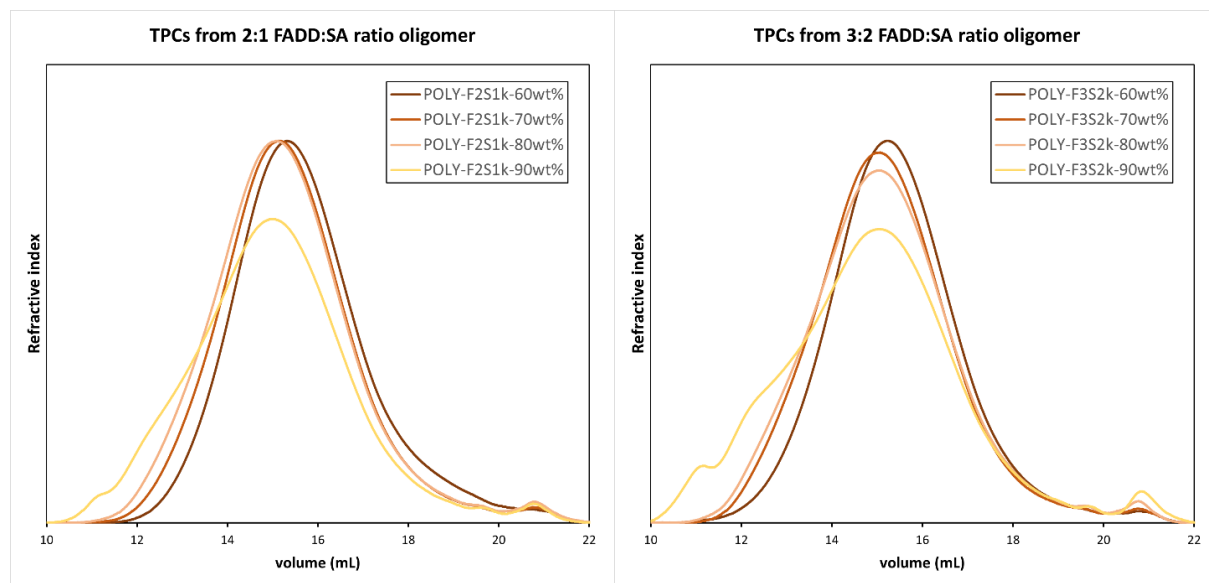


Figure 43: GPC data for polymers from (left) 2:1 ratio oligomers and (right) 3:2 ratio oligomers as soft blocks in different wt%

Table 9: Values for molecular mass from SEC Measurements from light scattering and refractive index detection for polymer samples

| entry | RI detection | | | Light scattering | | |
|------------------|-------------------|-------------------|------|-------------------|-------------------|------|
| | M_n (kg/mol) | M_w (kg/mol) | D | M_n (kg/mol) | M_w (kg/mol) | D |
| POLY-F2S1k-60wt% | 14.1 | 63.0 | 4.5 | 3.8 | 77.4 | 20.4 |
| POLY-F2S1k-70wt% | 16.6 | 81.0 | 4.9 | 10.4 | 94.6 | 9.1 |
| POLY-F2S1k-80wt% | 16.1 | 93.0 | 5.8 | 14.3 | 87.2 | 6.1 |
| POLY-F2S1k-90wt% | 17.7 | 139.3 | 7.9 | 28.7 | 156.8 | 5.5 |
| POLY-F3S2k-60wt% | 17.9 | 76.9 | 4.3 | 40.0 | 79.0 | 2.0 |
| POLY-F3S2k-70wt% | 19.4 | 95.8 | 4.9 | 46.3 | 107.0 | 2.3 |
| POLY-F3S2k-80wt% | 17.4 | 103.8 | 6.0 | 32.0 | 99.8 | 3.1 |
| POLY-F3S2k-90wt% | 14.7 | 181.6 | 12.4 | 73.0 | 280.9 | 3.9 |

The distributions are relatively broad with dispersities (D) higher than expected. This is consistent with what Karanastasis et al. saw in their SEC measurements of conventional step-growth, linear polymer architectures [4]. The oligomers influence this ratio by increasing the molecular weight dispersion of the final material. A larger amount of oligomer added will increase the dispersity, since the oligomer itself already has a larger distribution as can be seen from its SEC measurements. This can also be seen from the refractive index method for the 2:1 FADD:SA and 3:2 FADD:SA ratio and the light scattering method for the 3:2 FADD:SA ratio. However, the light scattering method for the 2:1 FADD:SA ratio shows reverse results. This can be explained by the defaults in the software's light scattering method. The POLY-F2S1k-90wt% and POLY-F3S2k-90wt% samples show a wider peak at lower volumes, as well as a bump at higher volumes. This can indicate that the polymers contain a fraction with higher molecular weight as well as some unreacted oligomers, which confirms the $^1\text{H-NMR}$ results at the 3.63 ppm peak. This can be caused by the difficult reaction to create a very homogenous mixture of PET

and the oligomer with such a high weight percentage of oligomer added, as explained in 2.2.3 Elongated soft segment. There might still be unreacted PET in the material as well, due to the miscibility of the TPC. For the other weight percentages of oligomers added in the polymer, the final polymers show that the peak becomes wider with every 10 wt% added. This is seen in the M_w/M_n ratio by using the refractive index method, which increases as well. The M_n and subsequently the M_w values increase as the amount of soft block increases, making it possible to form larger polymer chains as explained in 2.2.3 Elongated soft segment and Figure 15. On the other hand the molecular weight increases, more redistribution is necessary to create larger molecules, increasing the range of molecule sizes or the dispersity further.

4.3 Mechanical testing

4.3.1 DSC

A thermo-analytical characterization of the polymers is conducted using DSC analysis. Through DSC it is possible to determine the melting-, crystallization-, glass- and cold crystallization temperatures of a polymer. The difference in these temperatures is mostly depending on the soft block content in the TPC. The DSC graphs for the polymers with a differing SB wt% are given in Figure 12, with their corresponding values in Table 10.

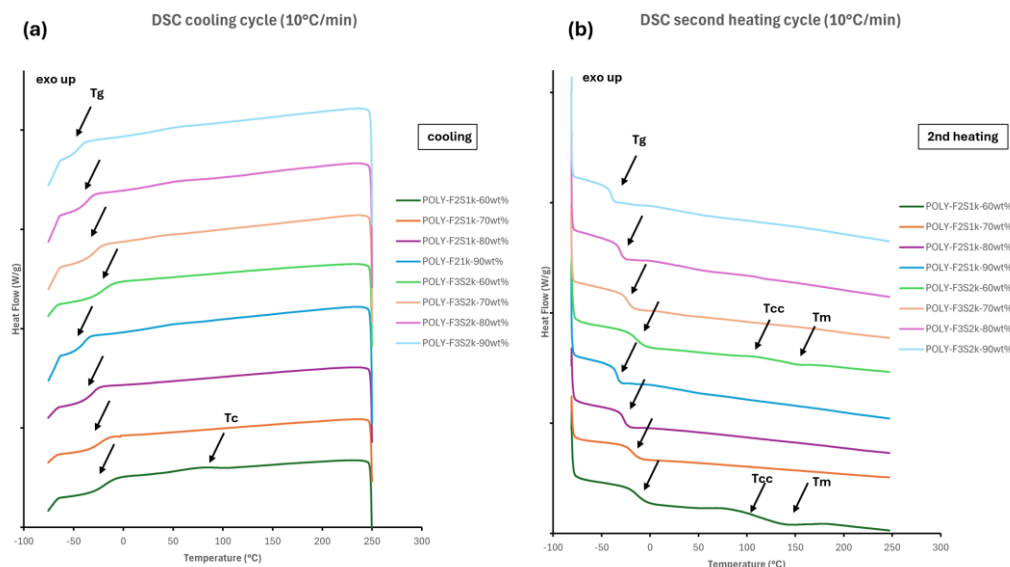


Figure 44: Thermograms of the polymers with 2:1 FADD:SA oligomer and 3:2 FADD:SA oligomer as soft blocks, showing (a) the cooling cycle (10°C/min) and (b) the second heating cycle (10°C/min). The graphs have been vertically adjusted for better clarity. Arrows mark the approximate locations of thermal transitions.

Table 10: Summary of thermal characterization of the polymers synthesized

| Sample | T_g (°C) | T_{cc} (°C) | ΔH_c (J/g) | T_c (°C) | ΔH_c (J/g) | T_m (°C) | ΔH_m (J/g) | $\alpha_c = \frac{\Delta H_m}{\Delta H_m^0}$ (%) |
|------------------|---------------|---------------|-----------------------|---------------|-----------------------|---------------|-----------------------|---|
| POLY-F2S1k-60wt% | -16.99 | 77.47 | 4.85 | 77.70 | 2.94 | 141.68 | 5.97 | 4.26 |
| POLY-F2S1k-70wt% | -20.7 | | | | | | | |
| POLY-F2S1k-80wt% | -28.65 | | | | | | | |
| POLY-F2S1k-90wt% | -36.27 | | | | | | | |
| POLY-F3S2k-60wt% | -16.88 | 107.20 | 1.165 | / | / | 151.19 | 1.19 | 0.85 |
| POLY-F3S2k-70wt% | -25.98 | | | | | | | |
| POLY-F3S2k-80wt% | -33.24 | | | | | | | |
| POLY-F3S2k-90wt% | -41.34 | | | | | | | |

Note: $\Delta H_m^0 = 140$ J/g [93]

Polymers with a SB wt% higher than 60, tend to be fully amorphous as they do not show any crystallization. The lack of a melting peak supports this theory, as melting is a characteristic first-order phase transition in crystalline substances, when there is no crystallization, melting is impossible. The decrease in the value of the T_g validates this even further. As the soft block has weaker intermolecular interactions that allow the polymer chains to move more freely at lower temperatures, compared to the hard block, the T_g is reduced with an increase in SB wt% because of the flexibility of the aliphatic FADD compound. Along with higher soft block weight percentages, the hard block becomes less prominent and has a lesser influence, further decreasing T_g . This effect of the soft block was already seen by Karanastasis A. et al. where a reduction of T_g (from -12 to -26°C) was observed when 49 to 66 wt% SB was incorporated in the TPC [3]. The crystallinity (α_c) can be calculated from the enthalpy values of the melting peak. At a wt% of 60, α_c gives a value of 4.26 % and 0.85 %, indicating that the upper limit of crystallization is almost met. It suggests nearly all of the crystalline regions that can form in the polymer have formed, and little room is left for additional crystallization. This is contrary to the theory that when the wt% of soft block increases, crystallization would increase because of the increasing hard block. The soft block is a more flexible segment, while the hard block is more rigid and can crystallize under certain conditions. A longer hard block, as a result of an elongated soft block, would show crystallinity, due to its potential to form ordered, crystalline structures. The T_c missing here with the higher SB wt%, confirms that the transesterification, as seen in 4.2.2. ^{13}C -NMR, occurs.

The samples with a higher amount of SB, also appear to be more transparent, as can be seen in Figure 45. This transparency indicates the polymers show mostly amorphous characteristics, as seen with the DSC measurements.

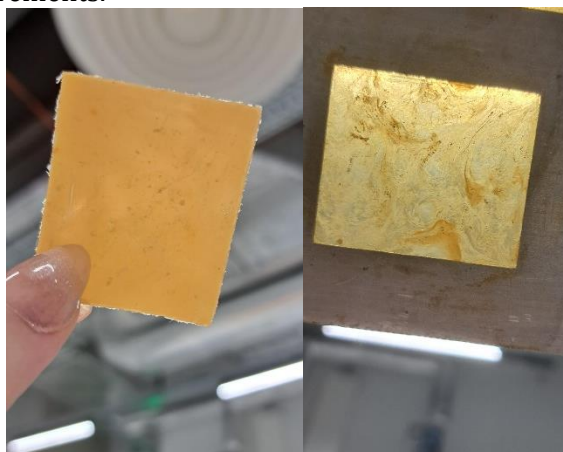


Figure 45: Appearance of synthesized polymers (left) with a 60 wt% of soft block (right) with a 80 wt% of soft block

4.3.2 Tensile testing

The mechanical properties of the TPCs are measured through tensile testing. The tensile tests for the polymers made with a 2:1 ratio oligomer are summarized in Figure 46 and Table 11.

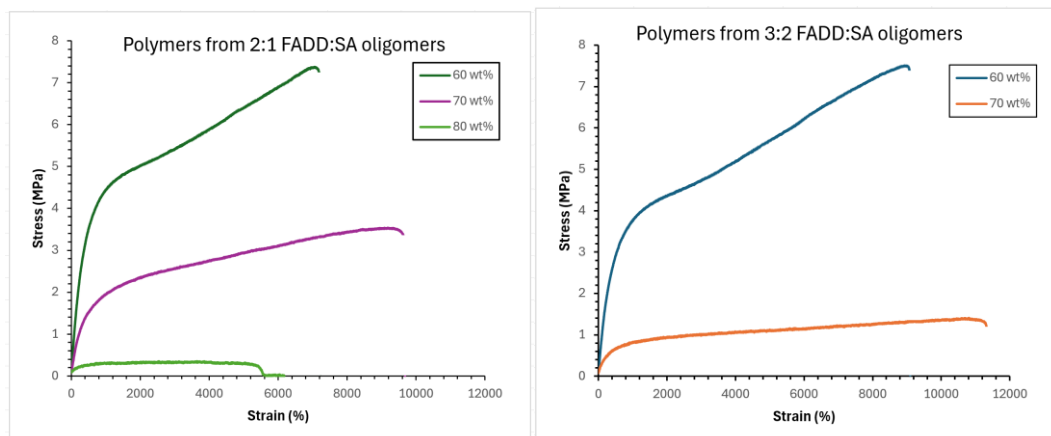


Figure 46: Summary of the stress-strain curves of the selected polymer samples derived from (left) 2:1 FADD:SA ratio oligomers (right) 3:2 FADD:SA ratio oligomers

Table 11: Summary of the mechanical properties of the selected polymer samples derived from 2:1 FADD:SA oligomers and 3:2 FADD:SA oligomers

| Polymer | E (N/mm ²) | Max Stress (MPa) | Strain at break (%) |
|------------|--------------------------|------------------|---------------------|
| POL-2:1-60 | 22.5 ± 1.5 | 6.6 ± 1.4 | 303.4 ± 161.4 |
| POL-2:1-70 | 11.7 ± 0.7 | 3.4 ± 0.5 | 362.8 ± 166.9 |
| POL-2:1-80 | 1.7 ± 0.3 | 0.3 ± 0.02 | 140.6 ± 15.3 |
| POL-3:2-60 | 17.4 ± 0.7 | 7.5 ± 0.6 | 512.0 ± 91.0 |
| POL-3:2-70 | 5.2 ± 0.5 | 1.4 ± 0.1 | 537.2 ± 53.3 |

Polymers with 90 SB wt% (POLY-F2S1k-90wt% and POLY-F3S2k-90wt%), and POLY-F3S2k-80wt%, are too tacky to perform tensile tests. The POLY-F2S1k-90wt% will be used to test their adhesive strength as described in 4.3.3 Adhesion tests. From the values for the Young's modulus (E), a decrease from 22.5 to 1.74 N/mm² can be seen when the SB wt% increases from 60 to 80. The same trend occurs with the POLY-F3S2k-60wt% and POLY-F3S2k-70wt%. However, POLY-F3S2k-60wt% shows already a lower value for E compared to POLY-F2S1k-60wt%. When the results from the tensile tests are compared to the results produced by Karanastasis A. et al. it is noticeable that their PET-60DFA sample has a maximum stress of 39.2 ± 3.7 MPa and strain at break of $811 \pm 43\%$, these are remarkably higher than the results from POLY-F2S1k-60wt% tested here with a maximum stress of 6.6 ± 1.4 and strain at break of $811 \pm 43\%$ [4]. The difference is following the results from the DSC. A higher crystallinity shows higher density in the packing of the molecular chains. Therefore, the material can be more stiff and show better strain and stress. When the soft block elongates and therefore, the hard block as well, the polymer generally becomes more ductile and flexible. Increases in strain at break and decreases in tensile strength and stiffness were expected, due to transesterification. Transesterification by ethylene glycol disrupts the crystalline structure, further reducing tensile strength and stiffness while increasing flexibility and ductility. As the polymers decrease both the strain at break, and the maximum stress, it may indicate that the transesterification effects increase the randomness and lead to a weaker material. This is in accordance with the results in 4.2.1 ¹H-NMR and 4.2.2. ¹³C-NMR.

4.3.3 Adhesion tests

Since materials with high wt% of soft block, show a sticky behavior, adhesion tests are conducted as described in 3.2.3 Characterization of the polymers - Methods. The results from this test conducted on a polymer with a 2:1 FADD:SA ratio oligomer in a 90wt%, are given in Figure 47.

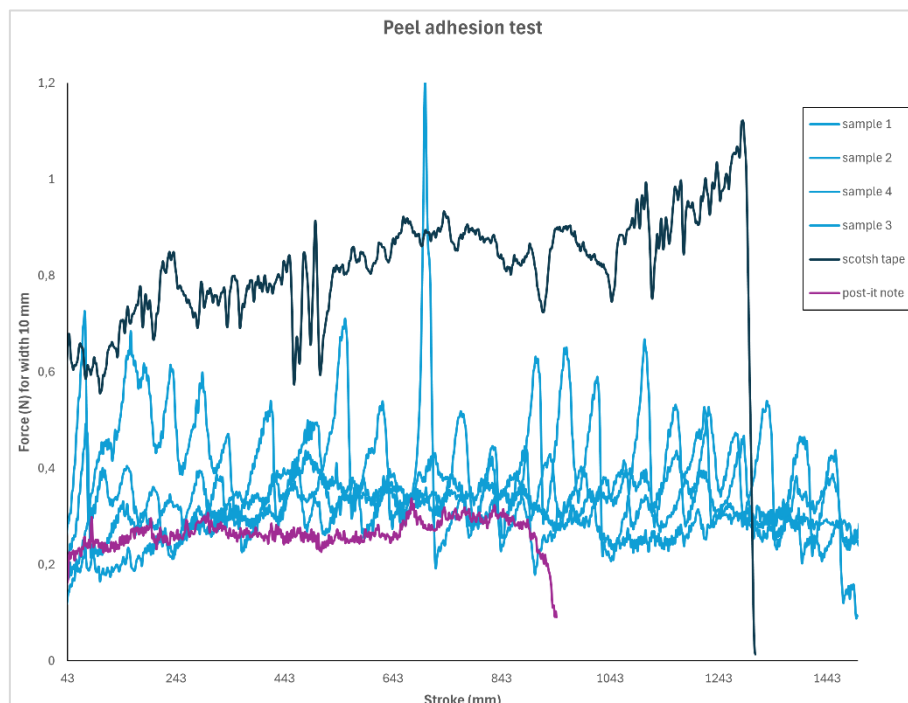


Figure 47: Peel adhesion test on POLY-2:1-90wt%, and for reference on scotch tape and a post-it note.

The values measured are given in Table 12.

Table 12: Values measured of sample POLY-F2S1k-90wt%, scotch tape and a sticky note during a peel adhesion test

| Sample number | Thickness (mm) | Weight (gf) | Max force (N) | Max stress (N/mm) |
|----------------------|-----------------------|--------------------|----------------------|--------------------------|
| Sample 1 | 10 | 25.10 | 0.53 | 0.05 |
| Sample 2 | 10 | 20.10 | 0.71 | 0.07 |
| Sample 3 | 10 | 19.10 | 1.08 | 0.11 |
| Sample 4 | 10 | 15.40 | 1.21 | 0.12 |
| Average | | | 0.88 | 0.09 |
| Stdev | | | 0.27 | 0.03 |
| Scotch tape | 20 | 1.00 | 2.24 | 0.11 |
| Post-it note | 10 | 1.00 | 0.34 | 0.03 |

For reference the same test is conducted on a piece of scotch tape and a post-it note, since these are well-known products. It is important to remark that the thickness and weight of the glue on these materials are unknown and might influence the results. In order to compare different adhesives it is advised to compare the maximum stress for a fair comparison accounting for the width of the adhesive bond. The average polymer sample has a maximum stress of 0.0880 N/mm which is slightly lower than the maximum stress of scotch tape being 0.1122 N/mm, but twice as high as the post-it note at 0.0338 N/mm. In fact, all of the polymer samples individually reported measurements higher than the post-it note, and, even one sample showed a maximum stress higher than the scotch tape. When the absolute load a material can handle, regardless of the bond width, is important, the scotch tape scores higher (2.2438 N) than the polymer samples (average of 0.8804 N). The post-it note shows a lower maximum force of 0.3376 N, which is lower than all individual polymer samples. None of the polymer samples left residue when peeled, making it a promising material for light gluing purposes such as tapes, sticky notes, and stickers.

5 Conclusion

Oligomer synthesis

A first important conclusion is that ^1H -NMR and GPC analyses confirmed that the expected oligomer structures were successfully formed. The use of a catalyst significantly improved the elongation of the oligomers, achieving optimal results when reaction conditions were set at 2 hours at 190°C under an argon atmosphere followed by 3 hours at 220°C under vacuum. Both 3:2 and 2:1 FADD:SA ratios proved to be effective. When no catalyst was added, longer reaction times and moderately higher temperatures were necessary to achieve similar elongation.

Polymer synthesis

The upcycling of PET into TPC materials with the use of the elongated FADD-SA oligomers is proved to be successful. However, transesterification, as evidenced by ^1H -NMR and ^{13}C -NMR, played a crucial role in rearranging the polymer chains, leading to the formation of additional repeating units alongside the expected ones. SEC Measurements confirm that transesterification occurs in the TPC material as seen from , leading to a broad range of molecular weights present, increasing the dispersity.

Characterization of Polymers

Thermomechanical analysis

DSC analysis revealed that increasing wt% of the soft block resulted in more amorphous materials, due to the disruption of the regular structure formation by transesterification. The materials become more transparent, as the crystallization is more inhibited when more soft block is added.

Table 13: Summary of thermomechanical analysis results of TPCs

| Sample | T_g ($^\circ\text{C}$) | T_{cc} ($^\circ\text{C}$) | ΔH_c (J/g) | T_c ($^\circ\text{C}$) | ΔH_c (J/g) | T_m ($^\circ\text{C}$) | ΔH_m (J/g) | $\alpha_c = \Delta H_m / \Delta H_m^0$ (%) |
|------------------|----------------------------|-------------------------------|--------------------|----------------------------|--------------------|----------------------------|--------------------|--|
| POLY-F2S1k-60wt% | -16.99 | 77.47 | 4.85 | 77.70 | 2.94 | 141.68 | 5.97 | 4.26 |
| POLY-F2S1k-70wt% | -20.7 | | | | | | | |
| POLY-F2S1k-80wt% | -28.65 | | | | | | | |
| POLY-F2S1k-90wt% | -36.27 | | | | | | | |
| POLY-F3S2k-60wt% | -16.88 | 107.20 | 1.165 | / | / | 151.19 | 1.19 | 0.85 |
| POLY-F3S2k-70wt% | -25.98 | | | | | | | |
| POLY-F3S2k-80wt% | -33.24 | | | | | | | |
| POLY-F3S2k-90wt% | -41.34 | | | | | | | |

Mechanical analysis

Tensile testing showed that higher soft block content decreased both the strain at break and the maximum stress, due to the increased randomness in the polymer chains. Additionally, materials with high soft block content exhibited a tacky, glue-like behavior.

Table 14: Summary of tensile test results on the TPCs

| Polymer | E (N/mm²) | Max Stress (MPa) | Strain at break (%) |
|----------------|--|-------------------------|----------------------------|
| POL-2:1-60 | 22.5 ± 1.5 | 6.6 ± 1.4 | 303.4 ± 161.4 |
| POL-2:1-70 | 11.7 ± 0.7 | 3.4 ± 0.5 | 362.8 ± 166.9 |
| POL-2:1-80 | 1.7 ± 0.3 | 0.3 ± 0.02 | 140.6 ± 15.3 |
| POL-3:2-60 | 17.4 ± 0.7 | 7.5 ± 0.6 | 512.0 ± 91.0 |
| POL-3:2-70 | 5.2 ± 0.5 | 1.4 ± 0.1 | 537.2 ± 53.3 |

The adhesion tests showed that the adhesion properties of the polymer are comparable to the well-known scotch tape, and better than a sticky note. It still needs to be taken into account that the thickness of the glue layer on the commercially available products are unknown, and might influence the results. However, the polymer material seems to be a good adhesive for light gluing purposes, and does not leave any residue when removed from a surface. The summary of the test results is given in table.

Table 15: Summary of peel adhesion test results

| Sample number | Max force (N) | Max stress (N/mm) |
|----------------------|----------------------|--------------------------|
| Av. Polymer | 0.8804 | 0.0880 |
| stdev | 0.2732 | 0.0273 |
| Scotch tape | 2.24376 | 0.11219 |
| Post-it note | 0.3376 | 0.03376 |

In summary, this research successfully elongated the soft blocks and incorporated PET upcycling methods to produce TPC materials. However, there is an extensive amount of transesterification during the polymerization. The outcome is not as expected, but the research provides insights in the behavior of the material and can be used to further research the elongation of soft blocks. For future research, it might be interesting to use new building blocks with more stable bonds such as amide bonds to create different compositions. By differing the soft block content, the material can be tailored to the desired properties. The resulting TPC materials from this research have potential applications in areas where properties such as flexibility and tackiness are desired, for example, bio-based reusable glue-like applications.

References

- [1] H. University. "About AFP." 2022.[Online]. Available: <https://www.uhasselt.be/en/onderzoeksgroepen-en/imo-imomec-afp/about-afp#anch-043-introduction-to-afp>. [Accessed February 2024].
- [2] H. University. "Research UHasselt." 2022.[Online]. Available: <https://www.uhasselt.be/en/onderzoeksgroepen-en/imo-imomec-afp/research#anch-upcycling-post-consumer-plastics-to-high-value-materials>. [Accessed February, 2024].
- [3] A. A. Karanastasis, V. Safin, and L. M. Pitet, "Bio-Based Upcycling of Poly(ethylene terephthalate) Waste for the Preparation of High-Performance Thermoplastic Copolyesters," *Macromolecules*, vol. 55, no. 3, pp. 1042-1049, 2022/02/08, doi: 10.1021/acs.macromol.1c02338.
- [4] A. A. Karanastasis, V. Safin, S. Damodaran, and L. M. Pitet, "Utility of Chemical Upcycling in Transforming Postconsumer PET to PBT-Based Thermoplastic Copolyesters Containing a Renewable Fatty-Acid-Derived Soft Block," *ACS Polymers Au*, vol. 2, no. 5, pp. 351-360, 2022/10/12 2022, doi: 10.1021/acspolymersau.2c00019.
- [5] R. Geyer, "A Brief History of Plastics," in *Mare Plasticum - The Plastic Sea: Combatting Plastic Pollution Through Science and Art*, M. Streit-Bianchi, M. Cimadevila, and W. Trettnak Eds. Cham: Springer International Publishing, 2020, pp. 31-47.
- [6] R. Geyer, J. R. Jambeck, and K. L. Law, "Production, use, and fate of all plastics ever made," *Science Advances*, vol. 3, no. 7, p. e1700782, 2017, doi: doi:10.1126/sciadv.1700782.
- [7] M. Shen, W. Huang, M. Chen, B. Song, G. Zeng, and Y. Zhang, "(Micro)plastic crisis: Unignorable contribution to global greenhouse gas emissions and climate change," *Journal of Cleaner Production*, vol. 254, p. 120138, 2020/05/01/ 2020, doi: 10.1016/j.jclepro.2020.120138.
- [8] U. S. government. "Overview of Greenhouse Gases." [Online]. Available: <https://www.epa.gov/ghgemissions/overview-greenhouse-gases>. [Accessed March, 2024].
- [9] M. Garside. "Annual production of plastics worldwide from 1950 to 2022." [Online]. Available: <https://www.statista.com/statistics/282732/global-production-of-plastics-since-1950/#:~:text=The%20worldwide%20production%20of%20plastics,percent%20from%20the%20previous%20year>. [Accessed March, 2024].
- [10] C. Bremer. "Plastic pollution is growing relentlessly as waste management and recycling fall short." [Online]. Available: <https://www.oecd.org/environment/plastic-pollution-is-growing-relentlessly-as-waste-management-and-recycling-fall-short.html>. [Accessed March, 2024].
- [11] R. Hale, M. Seeley, M. La Guardia, L. Mai, and E. Zeng, "A Global Perspective on Microplastics," *Journal of Geophysical Research: Oceans*, vol. 125, 01/14 2020, doi: 10.1029/2018JC014719.
- [12] H. Bouwmeester, P. C. H. Hollman, and R. J. B. Peters, "Potential Health Impact of Environmentally Released Micro- and Nanoplastics in the Human Food Production Chain: Experiences from Nanotoxicology," *Environmental Science & Technology*, vol. 49, no. 15, pp. 8932-8947, 2015/08/04 2015, doi: 10.1021/acs.est.5b01090.
- [13] A. Cózar *et al.*, "Plastic debris in the open ocean," *Proceedings of the National Academy of Sciences*, vol. 111, no. 28, pp. 10239-10244, 2014, doi: doi:10.1073/pnas.1314705111.
- [14] Fnf Research. "Polyethylene Terephthalate (PET) Market Size, Share Global Analysis Report, 2022-2030." 2022. [Online]. Available: <https://www.fnfresearch.com/polyethylene-terephthalate-pet-market#:~:text=In%202021%2C%20the%20annual%20production,and%20it%20can%20be%20recycled>. [Accessed March, 2024].

- [15] S. Sharifian and N. Asasian-Kolur, "Polyethylene terephthalate (PET) waste to carbon materials: Theory, methods and applications," *Journal of Analytical and Applied Pyrolysis*, vol. 163, p. 105496, 2022/05/01/ 2022, doi: 10.1016/j.jaap.2022.105496.
- [16] N. Roungpaisan *et al.*, "Effect of Recycling PET Fabric and Bottle Grade on r-PET Fiber Structure," *Polymers*, vol. 15, no. 10, p. 2330, 2023. [Online]. Available: <https://www.mdpi.com/2073-4360/15/10/2330>.
- [17] O. I. Nkwachukwu, C. H. Chima, A. O. Ikenna, and L. Albert, "Focus on potential environmental issues on plastic world towards a sustainable plastic recycling in developing countries," *International Journal of Industrial Chemistry*, vol. 4, no. 1, p. 34, 2013/07/22 2013, doi: 10.1186/2228-5547-4-34.
- [18] E. Commision. "Towards a true circular economy of PET plastics and textiles thanks to enzymatic recycling of waste." [Online]. Available: <https://webgate.ec.europa.eu/life/publicWebsite/project/LIFE20-ENV-FR-000596/towards-a-true-circular-economy-of-pet-plastics-and-textiles-thanks-to-enzymatic-recycling-of-waste>. [Accessed May,2024].
- [19] Textile Exchange. "Polyester is the most widely used fiber worldwide." [Online]. Available: <https://textileexchange.org/polyester/>. [Accessed March, 2024].
- [20] European Environment Agency of European Union. "Textiles." [Online]. Available: <https://www.eea.europa.eu/en/topics/in-depth/textiles#:~:text=In%202020%2C%20each%20person%20in,made%20of%20oil%20and%20gas>. [Aaccessed March, 2024].
- [21] X. Yuan, S. Li, S. Jeon, S. Deng, L. Zhao, and K. B. Lee, "Valorization of waste polyethylene terephthalate plastic into N-doped microporous carbon for CO₂ capture through a one-pot synthesis," *Journal of Hazardous Materials*, vol. 399, p. 123010, 2020/11/15/ 2020, doi: 10.1016/j.jhazmat.2020.123010.
- [22] K. De Clerck, H. Rahier, B. Van Mele, and P. Kiekens, "Thermal properties relevant to the processing of PET fibers," *Journal of Applied Polymer Science*, vol. 89, no. 14, pp. 3840-3849, 2003, doi: 10.1002/app.12543.
- [23] Y. Celik, M. Shamsuyeva, and H. J. Endres, "Thermal and Mechanical Properties of the Recycled and Virgin PET—Part I," *Polymers*, vol. 14, no. 7, p. 1326, 2022. [Online]. Available: <https://www.mdpi.com/2073-4360/14/7/1326>.
- [24] J. P. Jog, "Crystallization of Polyethylene terephthalate," *Journal of Macromolecular Science, Part C*, vol. 35, no. 3, pp. 531-553, 1995/08/01 1995, doi: 10.1080/15321799508014598.
- [25] L. Bartolome, M. Imran, B. G. Cho, A. A. Waheed, and D. H. Kim, "Recent Developments in the Chemical Recycling of PET," in *Material recycling:Trends and Perspectives*, D. S. Achilias Ed. Rijeka, Croatia: InTech, 2012, ch. 2, pp. 65-84.
- [26] Wikipedia. "Polyethylene terephthalate." [Online]. Available: https://en.wikipedia.org/wiki/Polyethylene_terephthalate. [Accessed August 5, 2024].
- [27] M. Jordi. "Typical Molecular Weights of Common Polymers." RQM+. [Online]. Available: [https://www.rqmplus.com/blog/typical-polymer-molecular-weights#:~:text=Polyethylene%20terephthalate%20\(PET\)%20is%20a,plastic%20bottle s%20for%20carbonated%20drinks](https://www.rqmplus.com/blog/typical-polymer-molecular-weights#:~:text=Polyethylene%20terephthalate%20(PET)%20is%20a,plastic%20bottle s%20for%20carbonated%20drinks). [Accessed August 5, 2024].
- [28] I. Cusano, L. Campagnolo, M. Aurilia, S. Costanzo, and N. Grizzuti, "Rheology of Recycled PET," (in eng), *Materials (Basel)*, vol. 16, no. 9, Apr 25 2023, doi: 10.3390/ma16093358.
- [29] Wankai Global. "Understanding Pet Grades: Film, Bottle, and Textile." [Online]. Available: <https://wkaiglobal.com/blogs/understanding-pet-grades-film-bottle-and-textile>. [Accessed August 5, 2024].
- [30] Omnexus. "Polyethylene terephthalate (PET) Manufacturers and Suppliers." [Online]. Available: <https://omnexus.specialchem.com/selection-guide/polyethylene-terephthalate-pet-plastic/suppliers>. [Accessed August 5, 2024].
- [31] PET Europe. "Members." [Online]. Available: <https://www.pet-europe.org/members/>. [accessed August 5, 2024].

- [32] S. M. Al-Salem, P. Lettieri, and J. Baeyens, "The valorization of plastic solid waste (PSW) by primary to quaternary routes: From re-use to energy and chemicals," *Progress in Energy and Combustion Science*, vol. 36, no. 1, pp. 103-129, 2010/02/01/ 2010, doi: 10.1016/j.pecs.2009.09.001.
- [33] I. A. Ignatyev, W. Thielemans, and B. Vander Beke, "Recycling of Polymers: A Review," *ChemSusChem*, vol. 7, no. 6, pp. 1579-1593, 2014, doi: 10.1002/cssc.201300898.
- [34] D. S. Gabriel, "How to increase plastic waste acceptance for mechanical recycling: introduction to material value conservation and its phenomenon," *Key Engineering Materials*, vol. 705, pp. 362-367, 2016, doi: 10.4028/www.scientific.net/kem.705.362.
- [35] N. Thachnatharen, S. Shahabuddin, and N. Sridewi, "The Waste Management of Polyethylene Terephthalate (PET) Plastic Waste: A Review," *IOP Conference Series: Materials Science and Engineering*, vol. 1127, no. 1, p. 012002, 2021/03/01 2021, doi: 10.1088/1757-899X/1127/1/012002.
- [36] L. Delva *et al.*, "Mechanical Recycling of Polymers for Dummies." [Online]. Available: <https://www.ugent.be/ea/match/cpmt/en/research/topics/circular-plastics/mechanicalrecyclingfordummiesv2.pdf>
- [37] W. Zhang *et al.*, "A critical review on secondary lead recycling technology and its prospect," *Renewable and Sustainable Energy Reviews*, vol. 61, pp. 108-122, 2016/08/01/ 2016, doi: 10.1016/j.rser.2016.03.046.
- [38] A. Rahimi and J. M. García, "Chemical recycling of waste plastics for new materials production," *Nature Reviews Chemistry*, vol. 1, no. 6, p. 0046, 2017/06/07 2017, doi: 10.1038/s41570-017-0046.
- [39] H. Li *et al.*, "Expanding plastics recycling technologies: chemical aspects, technology status and challenges," *Green Chemistry*, 10.1039/D2GC02588D vol. 24, no. 23, pp. 8899-9002, 2022, doi: 10.1039/D2GC02588D.
- [40] A. Schade, M. Melzer, S. Zimmermann, T. Schwarz, K. Stoewe, and H. Kuhn, "Plastic Waste Recycling—A Chemical Recycling Perspective," *ACS Sustainable Chemistry & Engineering*, 2024/07/01 2024, doi: 10.1021/acssuschemeng.4c02551.
- [41] H. Pilz, B. Brandt, and R. Fehringer, "The impact of plastics on life cycle energy consumption and greenhouse gas emissions in Europe," *Summary report June*, 2010.
- [42] K. Ragaert, L. Delva, and K. Van Geem, "Mechanical and chemical recycling of solid plastic waste," *Waste Management*, vol. 69, pp. 24-58, 2017/11/01/ 2017, doi: 10.1016/j.wasman.2017.07.044.
- [43] S. M. Al-Salem, P. Lettieri, and J. Baeyens, "Recycling and recovery routes of plastic solid waste (PSW): A review," *Waste Management*, vol. 29, no. 10, pp. 2625-2643, 2009/10/01/ 2009, doi: 10.1016/j.wasman.2009.06.004.
- [44] J. Hopewell, R. Dvorak, and E. Kosior, "Plastics recycling: challenges and opportunities," *Phil. Trans. R. Soc. B*, vol. 364, pp. 2115-2126, 2009, doi: 10.1098%2Frstb.2008.0311.
- [45] Plastics Europe. "Recycling technologies." [Online]. Available: <https://plasticseurope.org/sustainability/circularity/recycling/recycling-technologies/#:~:text=Mechanical%20recycling%20is%20the%20most,are%20relative%20easy%20to%20recycle>. [Accessed April, 2024].
- [46] Plastics Europe, "The circular economy for plastics: a European overview," Plastics Europe, 2020. [Online]. Available: https://plasticseurope.org/wp-content/uploads/2022/06/PlasticsEurope-CircularityReport-2022_2804-Light.pdf
- [47] "PET collection rates across Europe." [Online]. Available: <https://www.unesda.eu/pet-collection-rates/>. [Accessed August 5, 2024].
- [48] B. Santos. "Europe's PET bottles recycled content rate hits 24% in 2022," 2024. [Online]. Available: <https://www.sustainableplastics.com/news/europes-pet-bottles-recycled-content-rate-hits-24-2022>. [Accessed August 5, 2024].
- [49] ICIS, "PET market in Europe: State of play," 2022. [Online]. Available: https://www.unesda.eu/wp-content/uploads/2024/05/PET-plastic-Market-in-Europe-State-of-Play-Production-Collection-Recycling-Data_2022.pdf. [Accessed August 5, 2024].

- [50] D. E. Nikles and M. S. Farahat, "New Motivation for the Depolymerization Products Derived from Poly(Ethylene Terephthalate) (PET) Waste: a Review," *Macromolecular Materials and Engineering*, vol. 290, no. 1, pp. 13-30, 2005, doi: 10.1002/mame.200400186.
- [51] D. Carta, G. Cao, and C. D'Angeli, "Chemical recycling of poly(ethylene terephthalate) (pet) by hydrolysis and glycolysis," *Environmental Science and Pollution Research*, vol. 10, no. 6, pp. 390-394, 2003/11/01 2003, doi: 10.1065/espr2001.12.104.8.
- [52] C. N. Hoang, N. T. Nguyen, S. T. Ta, N. N. Nguyen, and D. Hoang, "Acidolysis of Poly(ethylene terephthalate) Waste Using Succinic Acid under Microwave Irradiation as a New Chemical Upcycling Method," *ACS Omega*, vol. 7, no. 50, pp. 47285-47295, 2022/12/20 2022, doi: 10.1021/acsomega.2c06642.
- [53] S. R. Shukla and A. M. Harad, "Aminolysis of polyethylene terephthalate waste," *Polymer Degradation and Stability*, vol. 91, no. 8, pp. 1850-1854, 2006/08/01/ 2006, doi: 10.1016/j.polymdegradstab.2005.11.005.
- [54] S. Bhatia, "Biodiesel," in *Advanced Renewable Energy Systems*, vol. 1. New Delhi, India: Woodhead Publishing, 2014, pp. 573-626.
- [55] Z. T. Laldinpui et al., "Methanolysis of PET Waste Using Heterogeneous Catalyst of Bio-waste Origin," *Journal of Polymers and the Environment*, vol. 30, no. 4, pp. 1600-1614, 2022/04/01 2022, doi: 10.1007/s10924-021-02305-0.
- [56] A. Sheel and D. Pant, "4 - Chemical Depolymerization of PET Bottles via Glycolysis," in *Recycling of Polyethylene Terephthalate Bottles*, S. Thomas, A. Rane, K. Kanny, A. V.K, and M. G. Thomas Eds.: William Andrew Publishing, 2019, pp. 61-84.
- [57] A. Aguado, L. Becerra, and L. Martínez, "Glycolysis optimisation of different complex PET waste with recovery and reuse of ethylene glycol," *Chemical Papers*, vol. 77, no. 6, pp. 3293-3303, 2023/06/01 2023, doi: 10.1007/s11696-023-02704-8.
- [58] A. Kulkarni, G. Quintens, and L. M. Pitet, "Trends in Polyester Upcycling for Diversifying a Problematic Waste Stream," *Macromolecules*, vol. 56, no. 5, pp. 1747-1758, 2023/03/14 2023, doi: 10.1021/acs.macromol.2c02054.
- [59] Diversitech Team. "Recycling vs Upcycling: What's the Difference?" 2022.[Online]. Available: <https://www.diversitech-global.com/post/recycling-vs-upcycling#:~:text=There%20are%20two%20main%20ways,than%20what%20they%20were%20before>. [Accessed March, 2024].
- [60] Z. Liu, H. Zhang, S. Liu, and X. Wang, "Bio-based upcycling of poly(ethylene terephthalate) waste to UV-curable polyurethane acrylate," *Polymer Chemistry*, 10.1039/D2PY01506D vol. 14, no. 10, pp. 1110-1116, 2023, doi: 10.1039/D2PY01506D.
- [61] N. A. Rorrer, S. Nicholson, A. Carpenter, M. J. Bidy, N. J. Grundl, and G. T. Beckham, "Combining Reclaimed PET with Bio-based Monomers Enables Plastics Upcycling," *Joule*, vol. 3, no. 4, pp. 1006-1027, 2019/04/17/ 2019, doi: 10.1016/j.joule.2019.01.018.
- [62] T. Tiso et al., "Towards bio-upcycling of polyethylene terephthalate," *Metabolic Engineering*, vol. 66, pp. 167-178, 2021/07/01/ 2021, doi: 10.1016/j.ymben.2021.03.011.
- [63] S. and P. Global. "Thermoplastic Copolyester Elastomers." [Online]. Available: <https://www.spglobal.com/commodityinsights/en/ci/products/copolyester-ether-chemical-economics-handbook.html>. [Accessed April,2020].
- [64] I. Bogachev, A. Vatulyan, V. Dudarev, and R. Nedin, "The investigation of the initial stress-strain state influence on mechanical properties of viscoelastic bodies," *PNRPU Mechanics Bulletin*, no. 2, pp. 15-24, 2019.
- [65] Y. Xu, Q. Zhang, Z. Wang, and L. Zhang, "Synthesis of novel thermoplastic polyester elastomers with biobased amorphous polyester as the soft segment," *Polymer Testing*, vol. 124, p. 108088, 2023/07/01/ 2023, doi: 10.1016/j.polymertesting.2023.108088.
- [66] Prismaneconsulting. "Global Thermoplastic Copolyesters (TPC) Market Demand & Forecast Analysis, 2016-2032." 2023. [Online]. Available: <https://medium.com/@prismaneconsulting265/global-thermoplastic-copolyesters-tpc-market-demand-forecast-analysis-2016-2032-8b1c43abb5a1>. [Accessed May, 2024].

- [67] R. J. Spontak and N. P. Patel, "Thermoplastic elastomers: fundamentals and applications," *Current Opinion in Colloid & Interface Science*, vol. 5, no. 5, pp. 333-340, 2000/11/01/ 2000, doi: 10.1016/S1359-0294(00)00070-4.
- [68] KRAIBURG TPE. "What is TPC material? Thermoplastic polyester elastomers." [Online]. Available: <https://www.kraiburg-tpe.com/en/what-tpc-material-thermoplastic-polyester-elastomers>. [Accessed May, 2024].
- [69] A. F. Sousa *et al.*, "Recommendations for replacing PET on packaging, fiber, and film materials with biobased counterparts," *Green Chemistry*, 10.1039/D1GC02082J vol. 23, no. 22, pp. 8795-8820, 2021, doi: 10.1039/D1GC02082J.
- [70] W. Zhou *et al.*, "Synthesis and characterization of bio-based poly(butylene furandicarboxylate)-b-poly(tetramethylene glycol) copolymers," *Polymer Degradation and Stability*, vol. 109, pp. 21-26, 2014/11/01/ 2014, doi: 10.1016/j.polymdegradstab.2014.06.018.
- [71] M. Gomes, A. Gandini, A. J. D. Silvestre, and B. Reis, "Synthesis and characterization of poly(2,5-furan dicarboxylate)s based on a variety of diols," *Journal of Polymer Science Part A: Polymer Chemistry*, vol. 49, no. 17, pp. 3759-3768, 2011, doi: 10.1002/pola.24812.
- [72] J. Zhu *et al.*, "Poly(butylene 2,5-furan dicarboxylate), a Biobased Alternative to PBT: Synthesis, Physical Properties, and Crystal Structure," *Macromolecules*, vol. 46, no. 3, pp. 796-804, 2013/02/12 2013, doi: 10.1021/ma3023298.
- [73] Circular Material Library. "BIO-PET." [Online]. Available: <https://circularmateriallibrary.org/material/bio-pet/>. [Accessed April, 2024].
- [74] A. Kulkarni, G. de Kort, G. Werumeus Buning, R. Ensink, and S. Rastogi, "Flexible and rigid block copolymers from recyclable polyesters," *European Polymer Journal*, vol. 213, p. 113086, 2024/06/10/ 2024, doi: 10.1016/j.eurpolymj.2024.113086.
- [75] Y. Nurhamiyah, A. Amir, M. Finnegan, E. Themistou, M. Edirisinghe, and B. Chen, "Wholly Biobased, Highly Stretchable, Hydrophobic, and Self-healing Thermoplastic Elastomer," *ACS Applied Materials & Interfaces*, vol. 13, no. 5, pp. 6720-6730, 2021/02/10 2021, doi: 10.1021/acsami.0c23155.
- [76] E. Gubbels, L. Jasinska-Walc, D. H. Merino, H. Goossens, and C. Koning, "Solid-State Modification of Poly(butylene terephthalate) with a Bio-Based Fatty Acid Dimer Diol Furnishing Copolyesters with Unique Morphologies," *Macromolecules*, vol. 46, no. 10, pp. 3975-3984, 2013/05/28 2013, doi: 10.1021/ma400559g.
- [77] A. A. Teran and N. P. Balsara, "Thermodynamics of Block Copolymers with and without Salt," *The Journal of Physical Chemistry B*, vol. 118, no. 1, pp. 4-17, 2014/01/09 2014, doi: 10.1021/jp408079z.
- [78] K. M. Hong and J. Noolandi, "Theory of phase equilibriums in systems containing block copolymers," *Macromolecules*, vol. 16, no. 7, pp. 1083-1093, 1983/07/01 1983, doi: 10.1021/ma00241a009.
- [79] C. R. McNeill, "Morphology of all-polymer solar cells," *Energy & Environmental Science*, 10.1039/C2EE03071C vol. 5, no. 2, pp. 5653-5667, 2012, doi: 10.1039/C2EE03071C.
- [80] C. C. Lin, S. V. Jonnalagadda, P. K. Kesani, H. J. Dai, and N. P. Balsara, "Effect of Molecular Structure on the Thermodynamics of Block Copolymer Melts," *Macromolecules*, vol. 27, no. 26, pp. 7769-7780, 1994/12/01 1994, doi: 10.1021/ma00104a035.
- [81] K. Hagita, T. Aoyagi, Y. Abe, S. Genda, and T. Honda, "Deep learning-based estimation of Flory-Huggins parameter of A-B block copolymers from cross-sectional images of phase-separated structures," *Scientific Reports*, vol. 11, no. 1, p. 12322, 2021/06/10 2021, doi: 10.1038/s41598-021-91761-8.
- [82] M. Gigli, A. Negroni, G. Zanaroli, N. Lotti, F. Fava, and A. Munari, "Environmentally friendly PBS-based copolyesters containing PEG-like subunit: Effect of block length on solid-state properties and enzymatic degradation," *Reactive and Functional Polymers*, vol. 73, no. 5, pp. 764-771, 2013/05/01/ 2013, doi: 10.1016/j.reactfunctpolym.2013.03.007.
- [83] C.-L. Xu, J.-B. Zeng, Q.-Y. Zhu, and Y.-Z. Wang, "Poly(ethylene succinate)-b-poly(butylene succinate) Multiblock Copolyesters: The Effects of Block Length and Composition on

- Physical Properties," *Industrial & Engineering Chemistry Research*, vol. 52, no. 38, pp. 13669-13676, 2013/09/25 2013, doi: 10.1021/ie4018379.
- [84] S. Fakirov and T. Gogeva, "Poly(ether/ester)s based on poly(butylene terephthalate) and poly(ethylene glycol), 1. Poly(ether/ester)s with various polyether: polyester ratios," *Die Makromolekulare Chemie*, vol. 191, no. 3, pp. 603-614, 1990, doi: 10.1002/macp.1990.021910315.
- [85] S. Fakirov and T. Gogeva, "Poly(ether/ester)s based on poly(butylene terephthalate) and poly(ethylene glycol), 2. Effect of polyether segment length," *Die Makromolekulare Chemie*, vol. 191, no. 3, pp. 615-624, 1990, doi: 10.1002/macp.1990.021910316.
- [86] H. J. Manuel and R. J. Gaymans, "Segmented block copolymers based on dimerized fatty acids and poly(butylene terephthalate)," *Polymer*, vol. 34, no. 3, pp. 636-641, 1993/01/01/ 1993, doi: 10.1016/0032-3861(93)90563-P.
- [87] R. J. Cella, "Morphology of segmented polyester thermoplastic elastomers," *Journal of Polymer Science: Polymer Symposia*, vol. 42, no. 2, pp. 727-740, 1973, doi: 10.1002/polc.5070420224.
- [88] J. Denny. "Biobased Succinic Acid: Is the Sustainable Route Becoming Economically Viable Once More?" [Online]. Available: <https://www.resourcewise.com/chemicals-blog/biobased-succinic-acid-is-the-sustainable-route-becoming-economically-viable-once-more> [Accessed April, 2024].
- [89] X. Wan *et al.*, "Facile Synthesis of Dimethyl Succinate via Esterification of Succinic Anhydride over ZnO in Methanol," *ACS Sustainable Chemistry & Engineering*, vol. 6, no. 3, pp. 2969-2975, 2018/03/05 2018, doi: 10.1021/acssuschemeng.7b02598.
- [90] L. He *et al.*, "One-pot synthesis of dimethyl succinate from d-fructose using Amberlyst-70 catalyst," *Molecular Catalysis*, vol. 508, p. 111584, 2021/05/01/ 2021, doi: 10.1016/j.mcat.2021.111584.
- [91] B. Gong *et al.*, "Quasi-Static and Tensile Behaviors of the Bamboos," in *Preprints*, ed: Preprints, 2017.
- [92] ZwickRoell. "Tear Growth, Peel, and Adhesion Characteristics." [Online]. Available: <https://www.zwickroell.com/industries/plastics/thin-sheeting-and-plastic-films/tear-growth-peel-and-adhesion-characteristics/>. [Accessed July 25, 2024].
- [93] T. L. Hanley, J. S. Forsythe, D. Sutton, G. Moad, R. P. Burford, and R. B. Knott, "Crystallisation kinetics of novel branched poly(ethylene terephthalate): a small-angle X-ray scattering study," *Polymer International*, vol. 55, no. 12, pp. 1435-1443, 2006, doi: 10.1002/pi.2097.

Appendix

Appendix 1

Ratio values for oligomers with varying reaction time between 1 hour and 7 hours.

Table 16: Ratio values calculated from ^1H NMR spectra of the oligomers with varying reaction times (1hours-7hours)

| Oligomer | Ratio value |
|--------------------|--------------------|
| <i>F2S1-1h-220</i> | 0.49 |
| <i>F2S1-2h-190</i> | 0.52 |
| <i>F2S1-4h-190</i> | 0.61 |
| <i>F2S1-5h-220</i> | 0.75 |
| <i>F2S1-6h-190</i> | 0.61 |
| <i>F2S1-7h-190</i> | 0.70 |

Appendix 2

^1H -NMR spectra of oligomers with and without addition of catalyst.

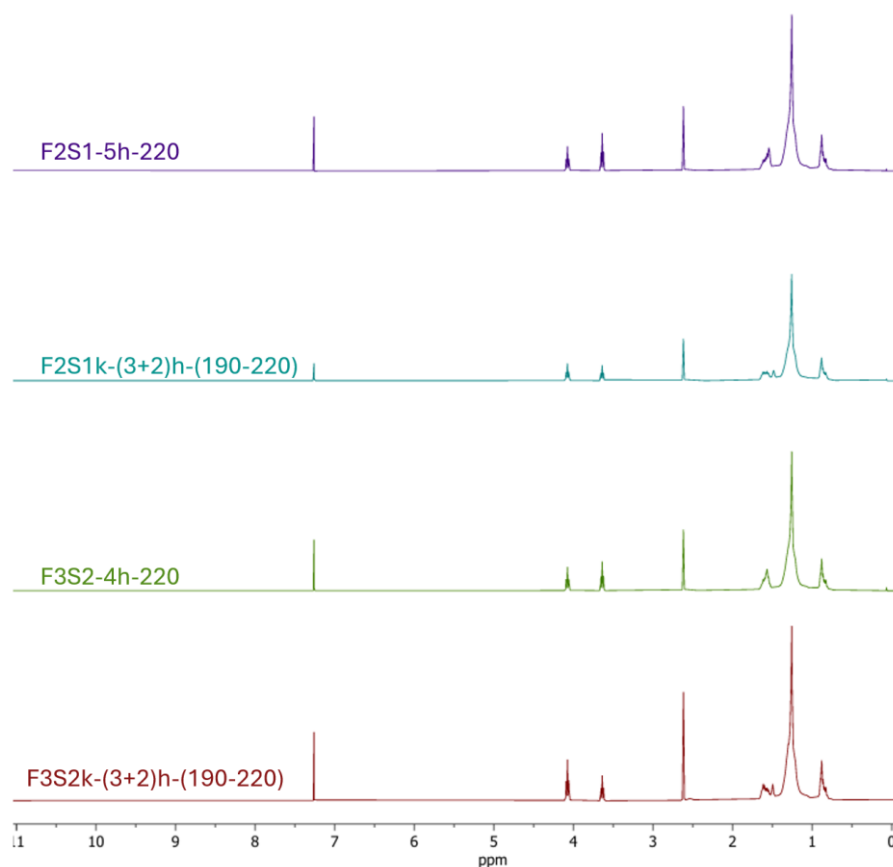


Figure 48: ^1H -NMR spectra of oligomers with and without addition of the catalyst. From top to bottom: (a) 2:1 FADD:SA ratio oligomer without catalyst (b) 2:1 FADD:SA ratio oligomer with catalyst (c) 3:2 FADD:SA oligomer without catalyst (d) 3:2 FADD:SA oligomer with catalyst

Appendix 3

^1H -NMR spectra of oligomers used for polymer synthesis.

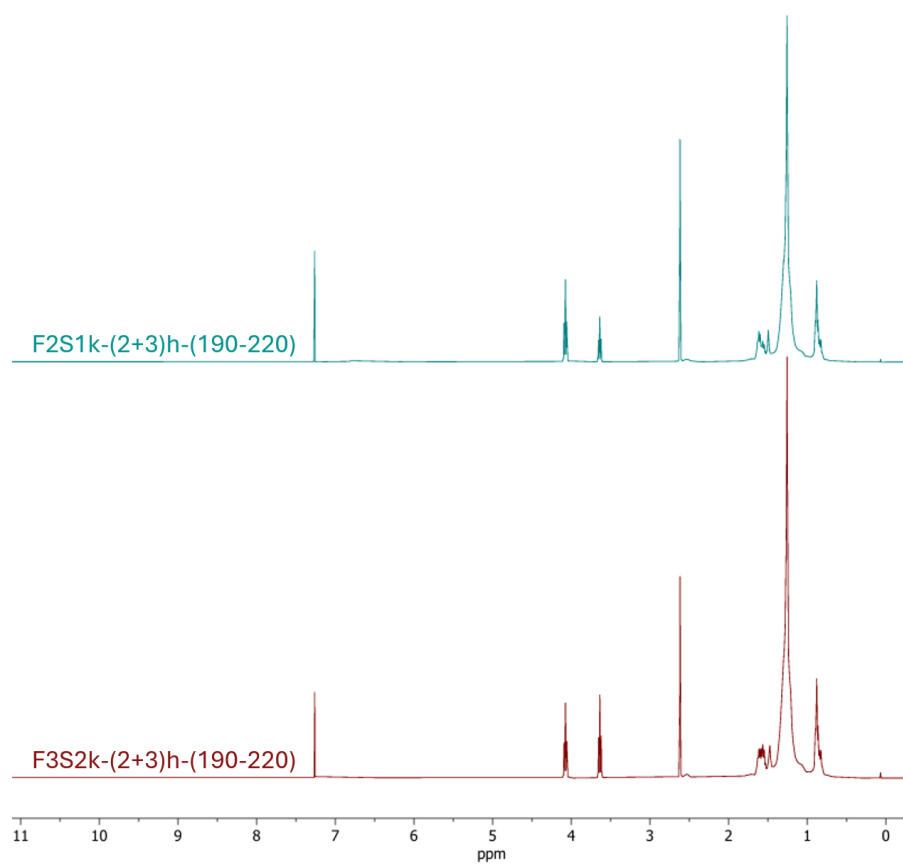


Figure 49: ^1H -NMR spectra of the oligomers used for the polymer synthesis (top) 2:1 FADD:SA ratio oligomer (bottom) 3:2 FADD:SA ratio oligomer

Appendix 4

^1H -NMR spectra of TPCs from different oligomers.

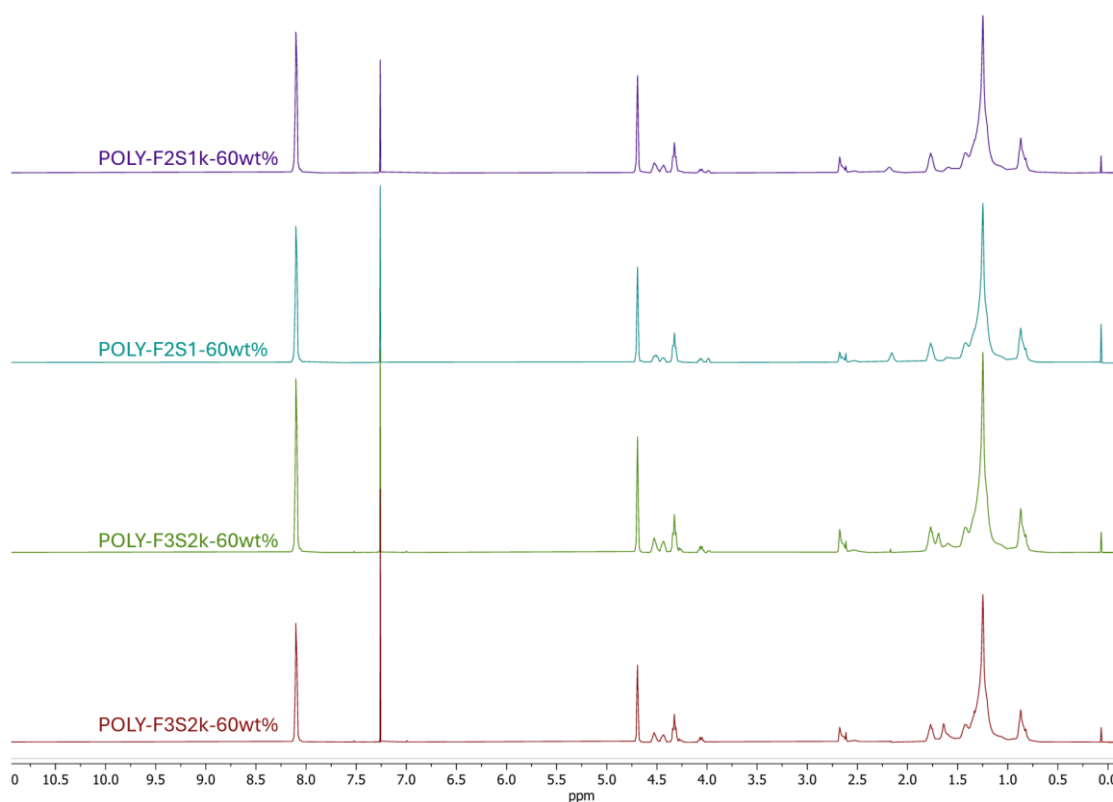


Figure 50: TPCs synthesized from different oligomers and different FADD:SA ratios

Appendix 5

Resulting values of ^1H -NMR spectra of polymers with different weight percentages.

Table 17: ^1H -NMR accompanying resulting values of spectra given in Figure 37.

| Peak | Integral of polymers with % wt of 2:1 oligomer SB | | | |
|------|---|--------|--------|--------|
| | 60 wt% | 70 wt% | 80 wt% | 90 wt% |
| a | 1.00 | 1.00 | 1.00 | 1.00 |
| b | 0.50 | 0.41 | 0.26 | 0.07 |
| c | 0.31 | 0.40 | 0.54 | 0.70 |
| d | 0.25 | 0.33 | 0.46 | 0.71 |
| FADD | 6.21 | 8.18 | 12.09 | 18.37 |
| Peak | Integral of polymers with % wt of 3:2 oligomer SB | | | |
| | 60 wt% | 70 wt% | 80 wt% | 90 wt% |
| a | 1.00 | 1.00 | 1.00 | 1.00 |
| b | 0.48 | 0.34 | 0.32 | 0.01 |
| c | 0.35 | 0.46 | 0.47 | 0.82 |
| d | 0.23 | 0.29 | 0.29 | 0.96 |
| FADD | 6.85 | 9.88 | 9.96 | 27.41 |